

CCSN using Machine Learning in multi-messenger context

Irene Di Palma

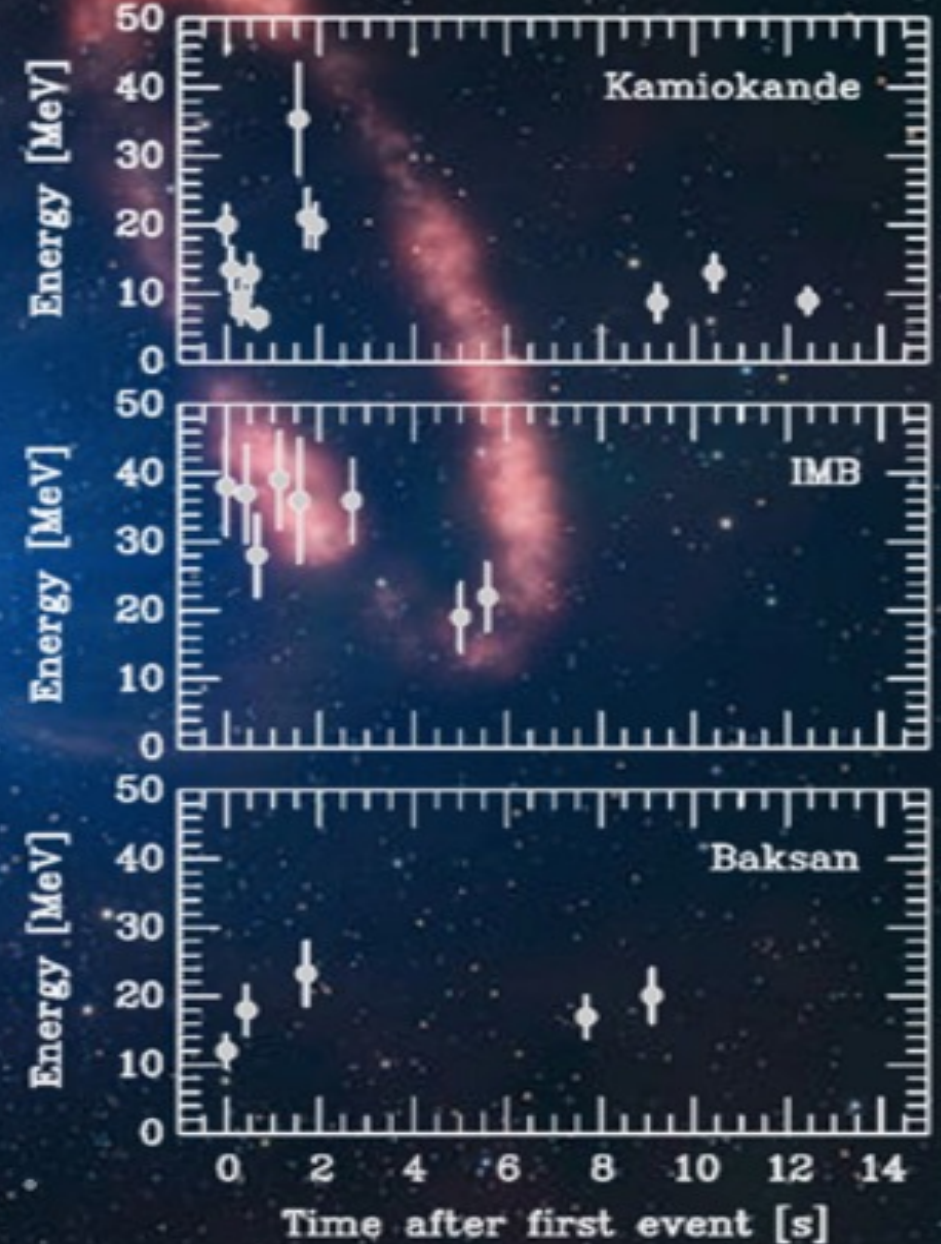
Sapienza University of Rome
Irene.DiPalma@roma1.infn.it



Motivations

- In a supernova explosion, GWs are generated in the inner core of the source, so that this messenger carries direct information of the inner mechanism.
- Although the phenomenon is among of the most energetic in the universe, the amplitude of the gravitational wave impinging on a detector on the Earth is extremely faint.
- For a CCSN in the center of the Milky way, a rare event, we could expect amplitudes of the metric tensor perturbations ranging between 10^{-21} – 10^{-23} .
- To increase the detection probability we should increase the volume of the universe to be explored and this can be achieved both by decreasing the detector noise and using better performing statistical algorithms.

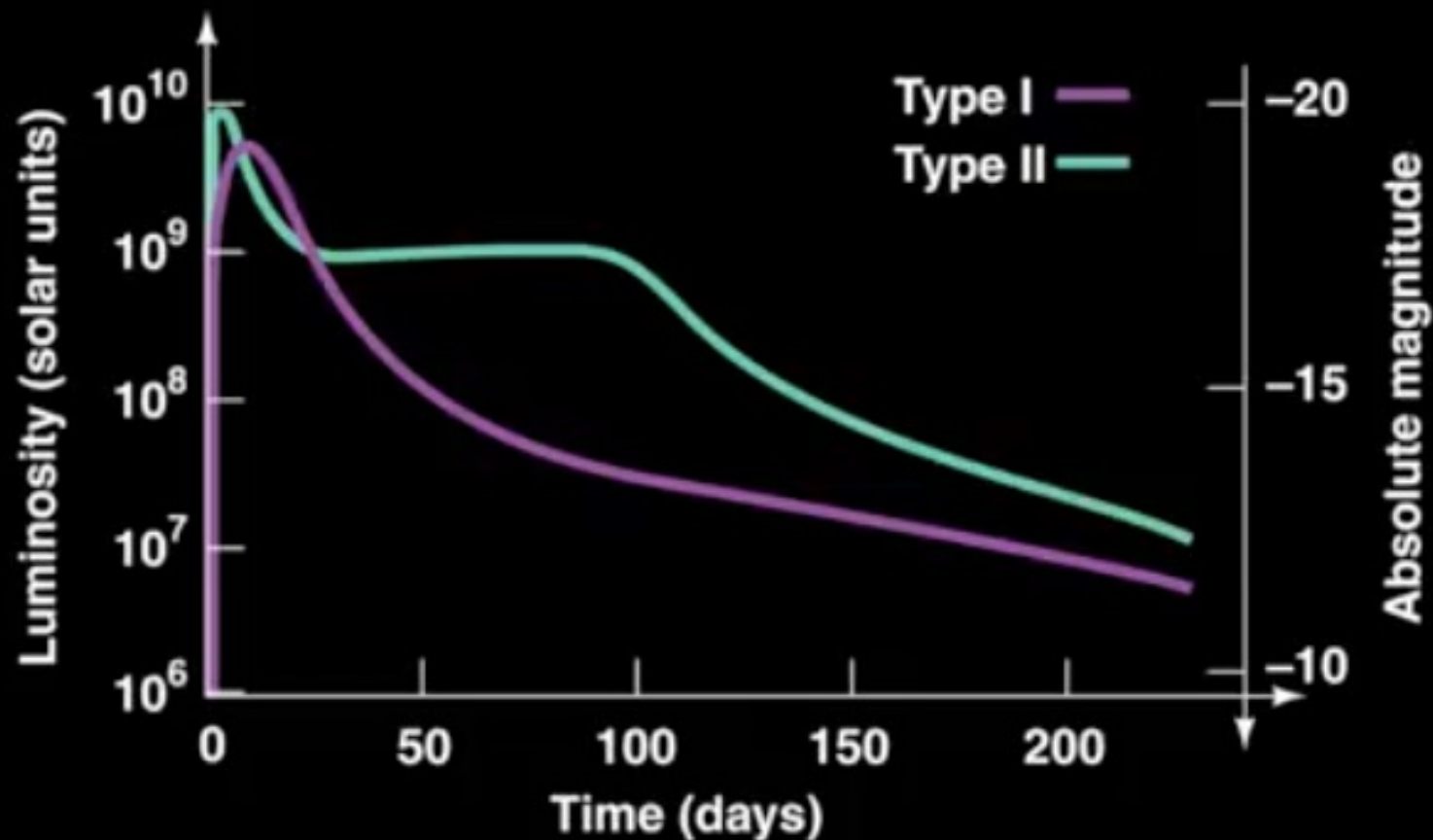
MeV Neutrinos from SN1987A



February 23, 1987.

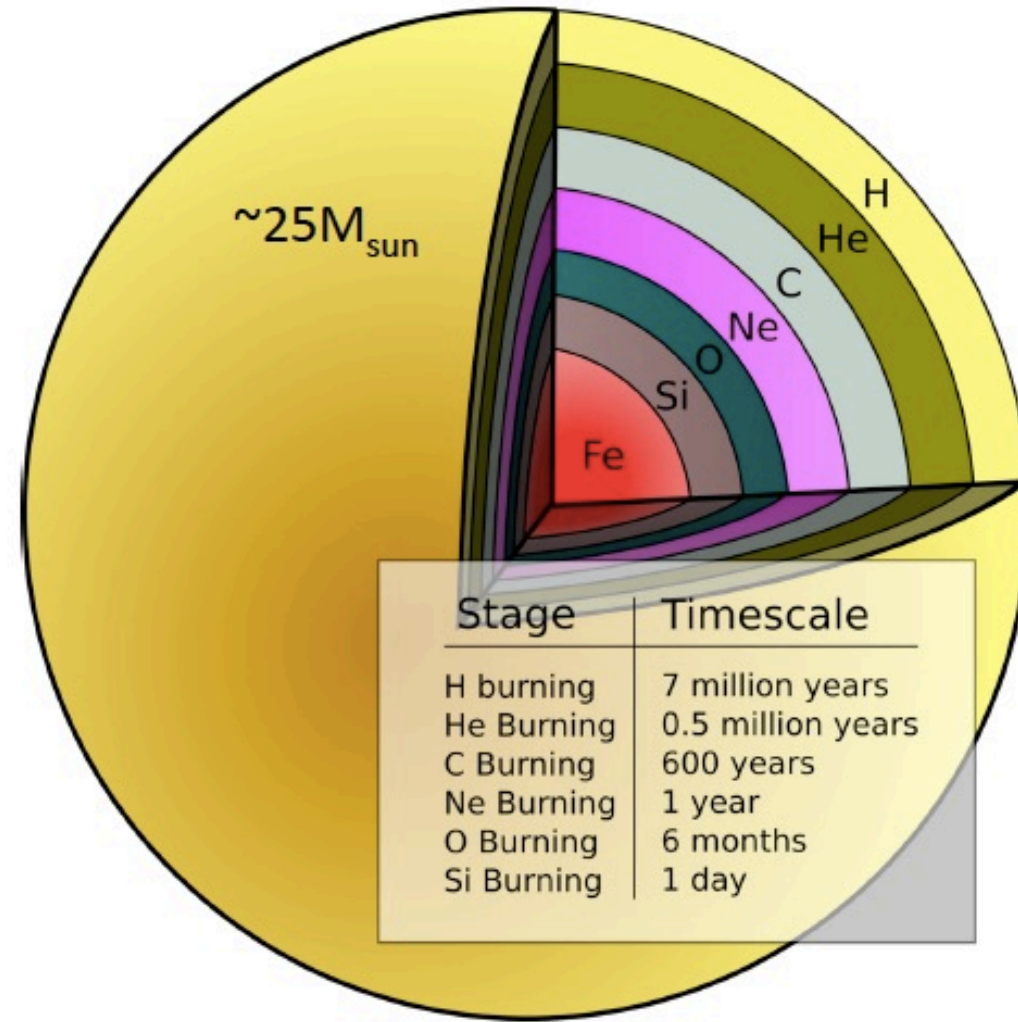
Supernovae

- **Thermonuclear Supernovae: Type Ia**
 - Caused by runaway thermonuclear burning of white dwarf fuel to Nickel
 - Roughly of 10^{51} ergs released
 - Very bright, used as standard candles
 - No remnant
- **Core Collapse Supernovae: Type II, Ib, Ic**
 - Result from the collapse of an iron core in an evolved massive star ($M_{ZAMS} > 8-10 M_{SUN}$)
 - Few $\times 10^{53}$ ergs released in gravitational collapse, most (99%) radiated in neutrinos
 - Spread stellar evolution elemental products throughout galaxy
 - Neutron star or black hole remnant



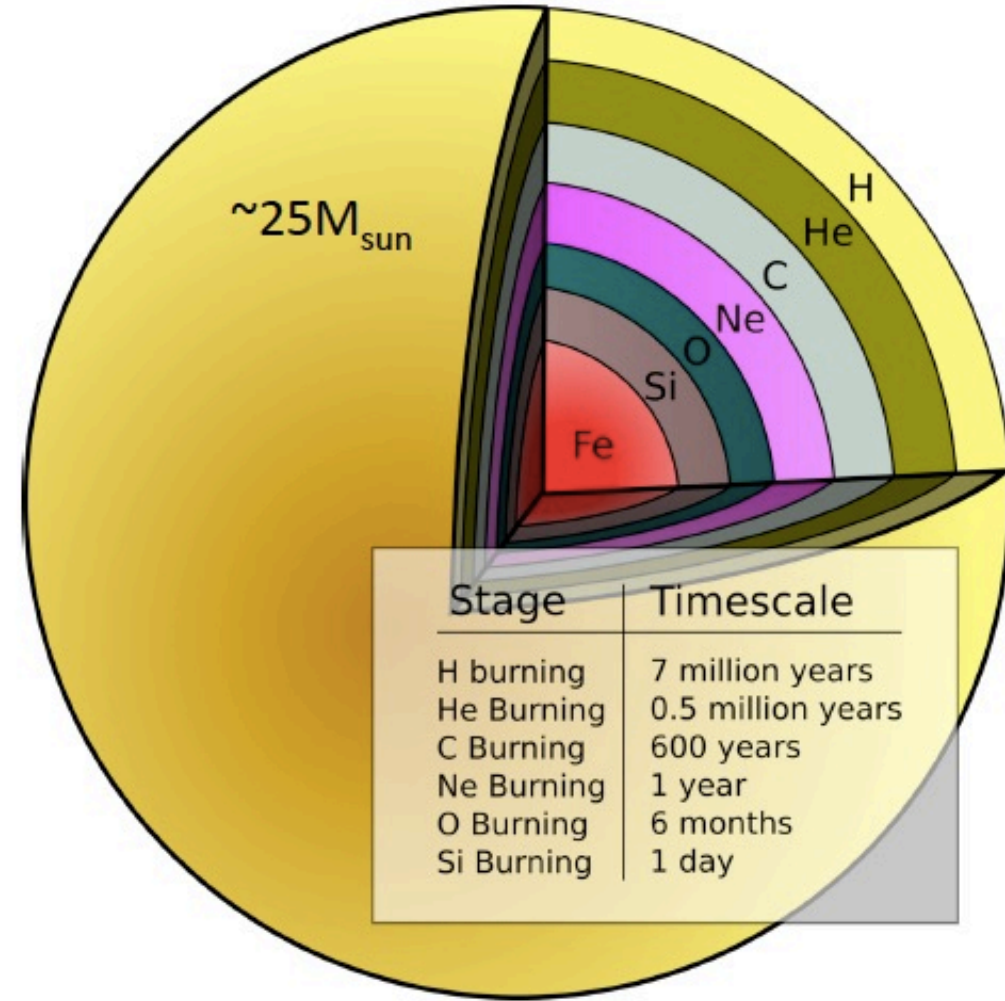
Massive Stars: Burning stages

- Stars spend most of their lives burning hydrogen.
- The product – helium – settles in the core and will burn when temperatures increase sufficiently.
- For massive stars ($M > 8-10M_{\text{sun}}$), the process continues through carbon, oxygen, ... , up to iron.
- This process does not continue past iron as iron is one of the most tightly bound nuclei.
- Iron core builds up in center of star.



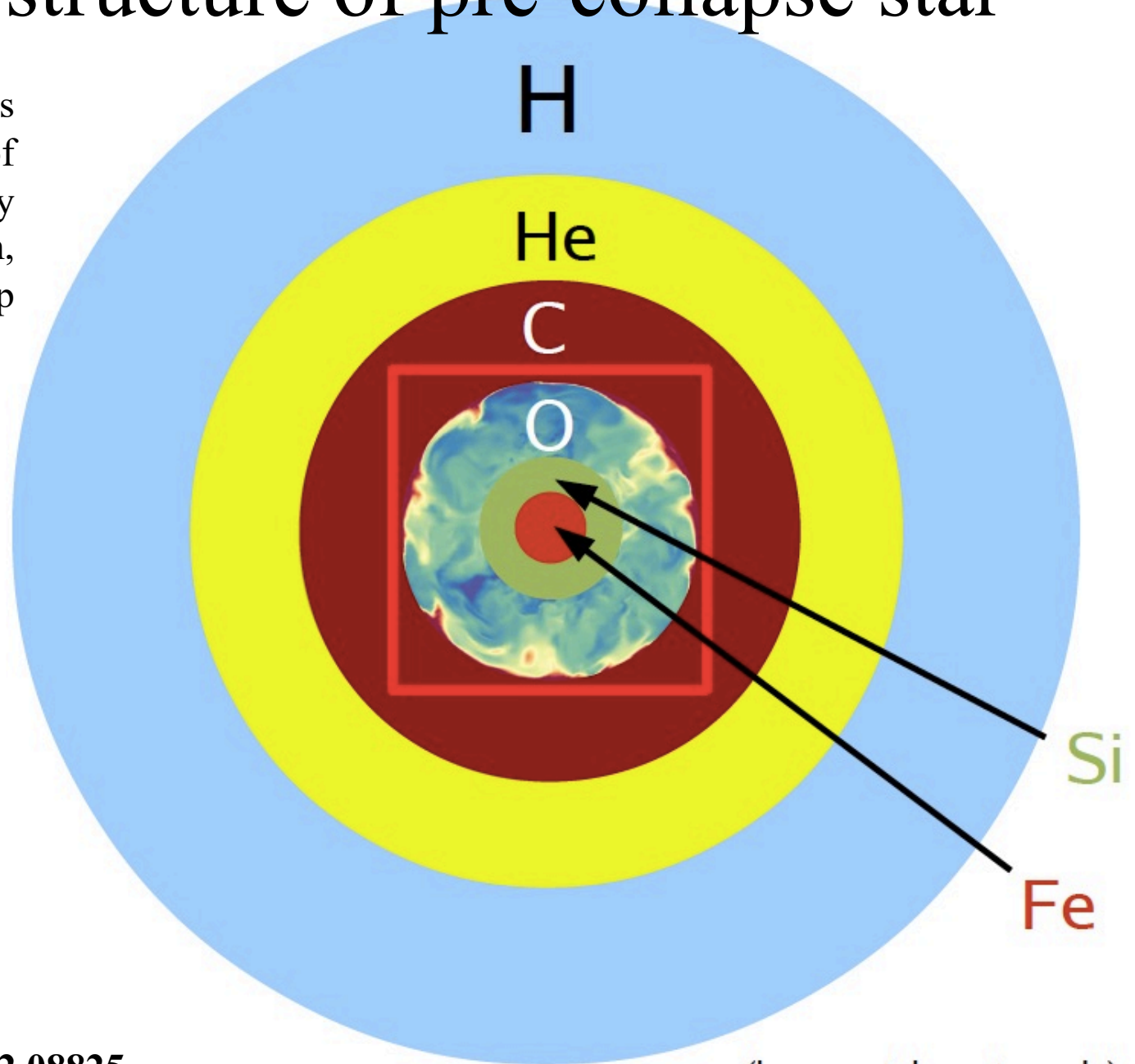
Massive Stars: End Stage

- Stars are, for the majority of the time, in hydrostatic equilibrium because the radiation pressure of the photons from nuclear reactions balance gravity.
- Iron cores however are supported by electron degeneracy pressure, much like a white dwarf, there is a maximum mass that electron degeneracy pressure can support.



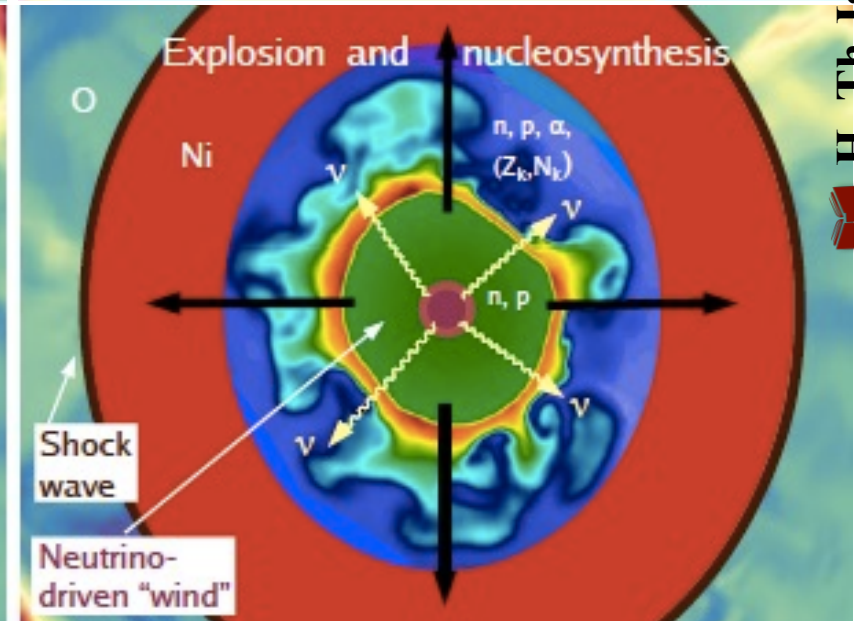
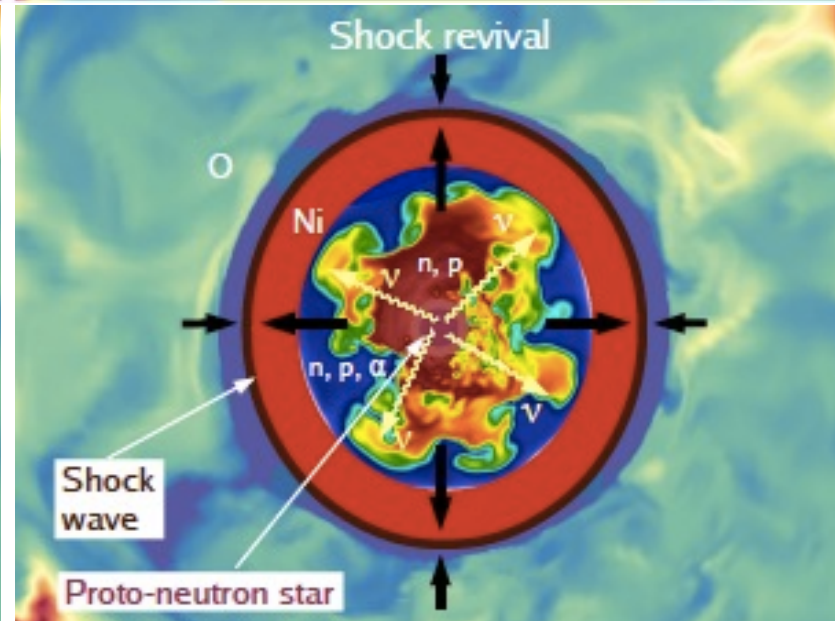
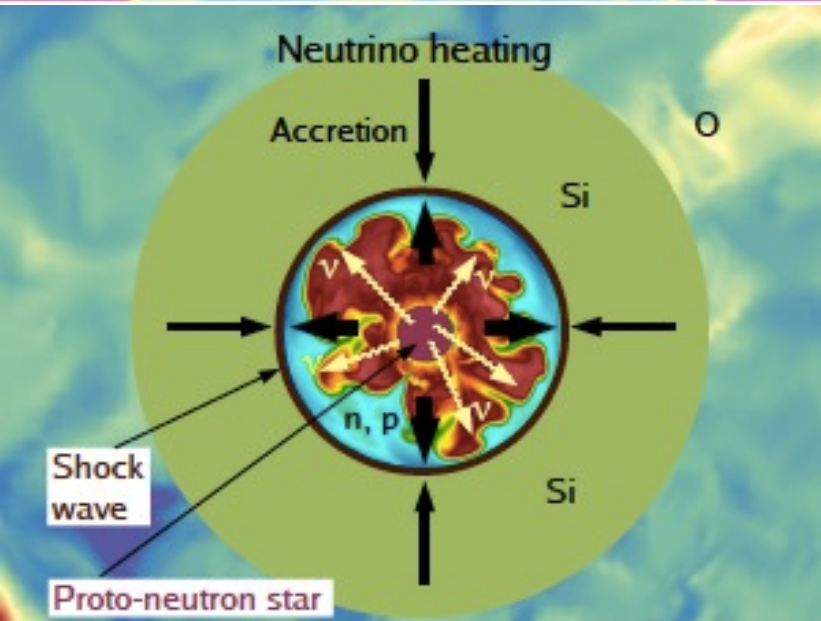
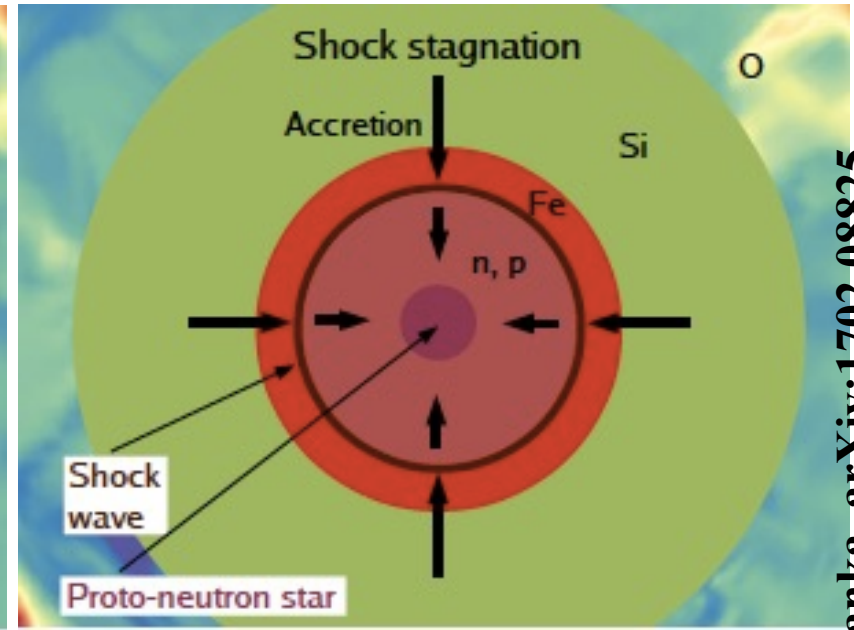
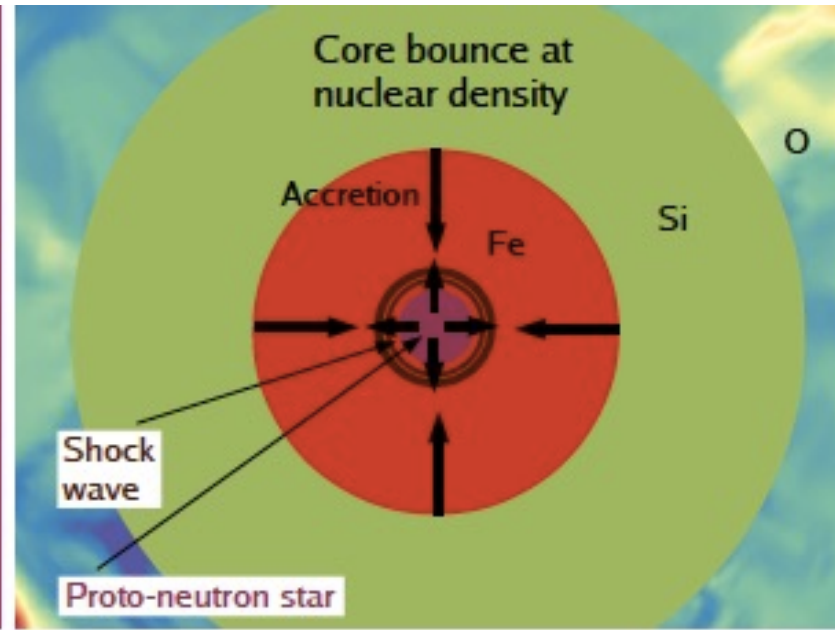
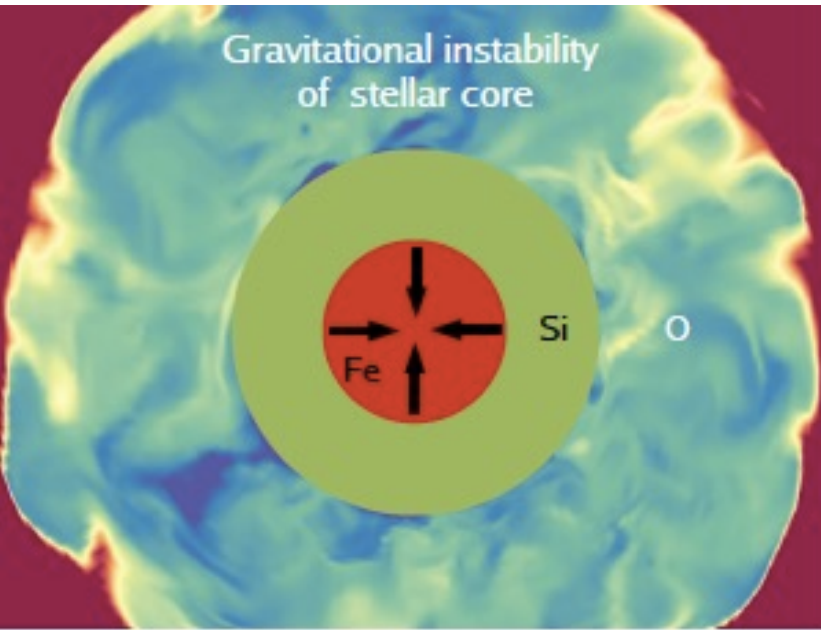
Onion shell structure of pre-collapse star

Shells of progressively heavier elements contain the ashes of a sequence of nuclear burning stages, which finally build up a degenerate core of oxygen, neon and magnesium or iron-group elements at the center.

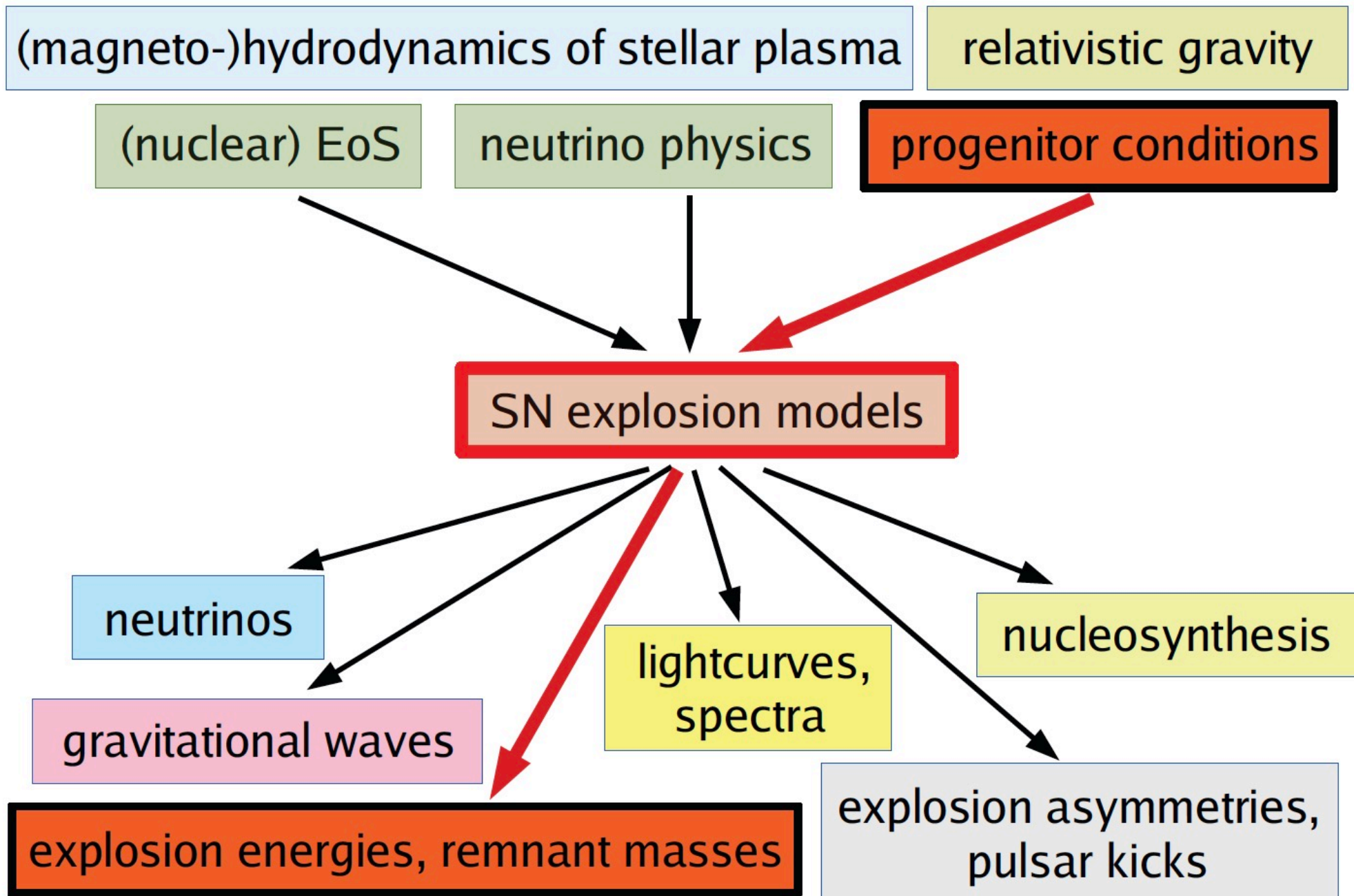


Convective burning can lead to large scale velocity and density perturbations in the oxygen and silicon layers (as indicated for the O-shell).

Dynamical phases of stellar core collapse and explosion



Predictions of Signals from Supernovae



A new gravitational wave signature from standing accretion shock instabilities in supernovae

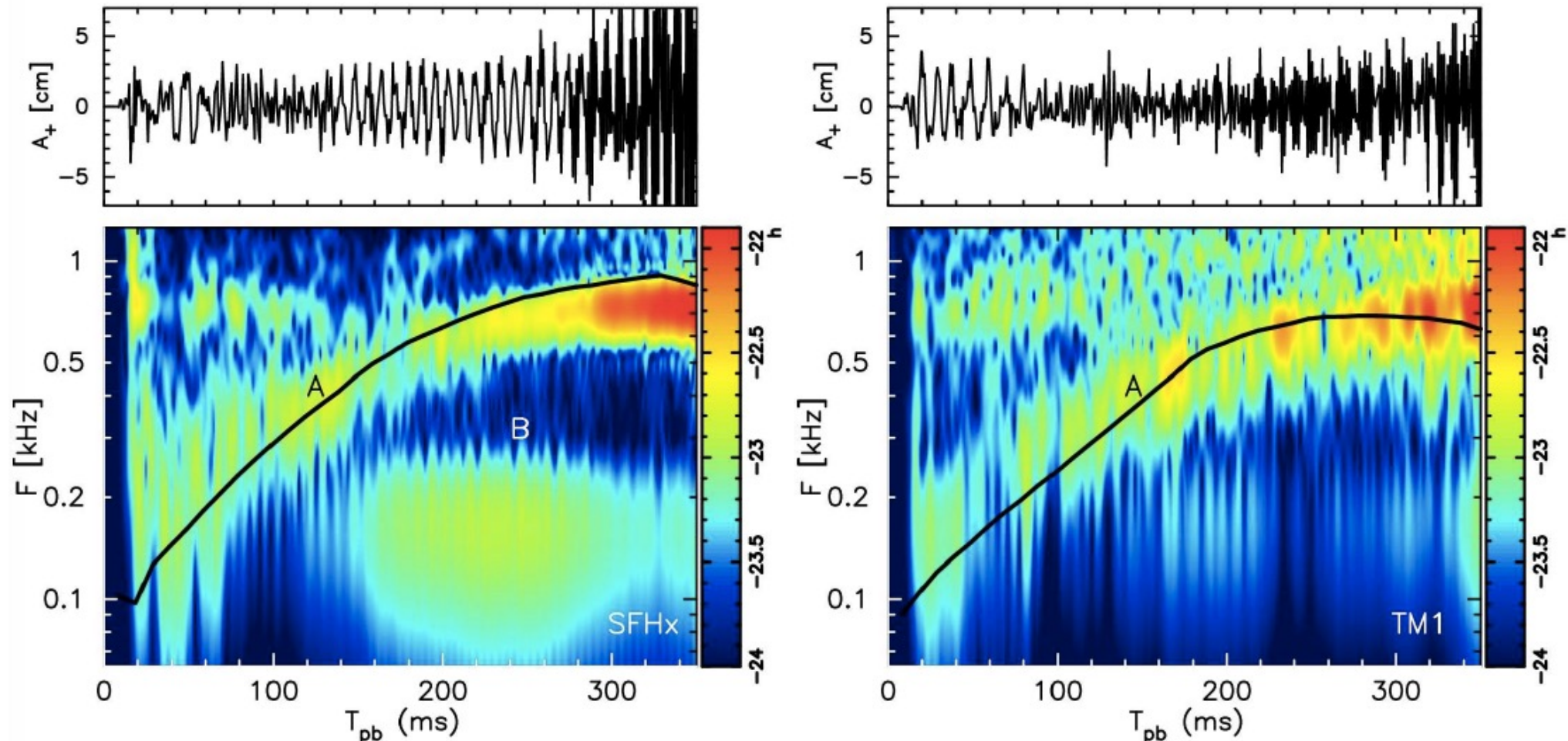
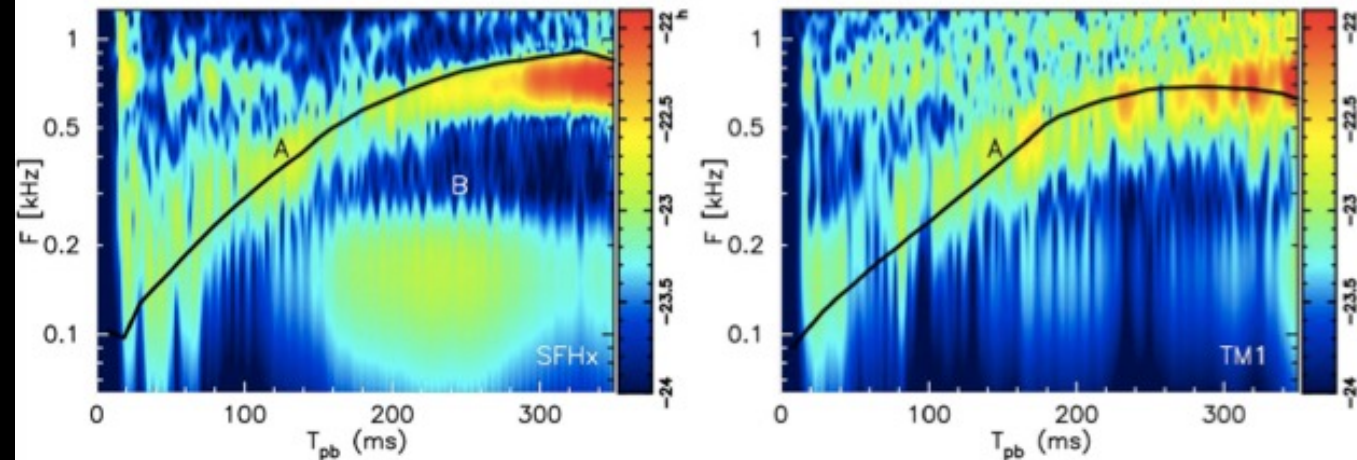


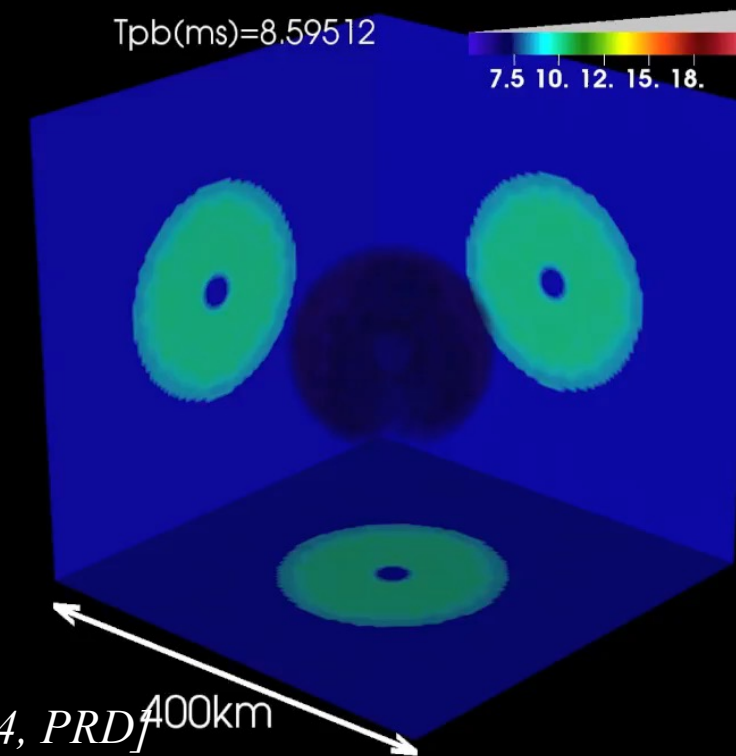
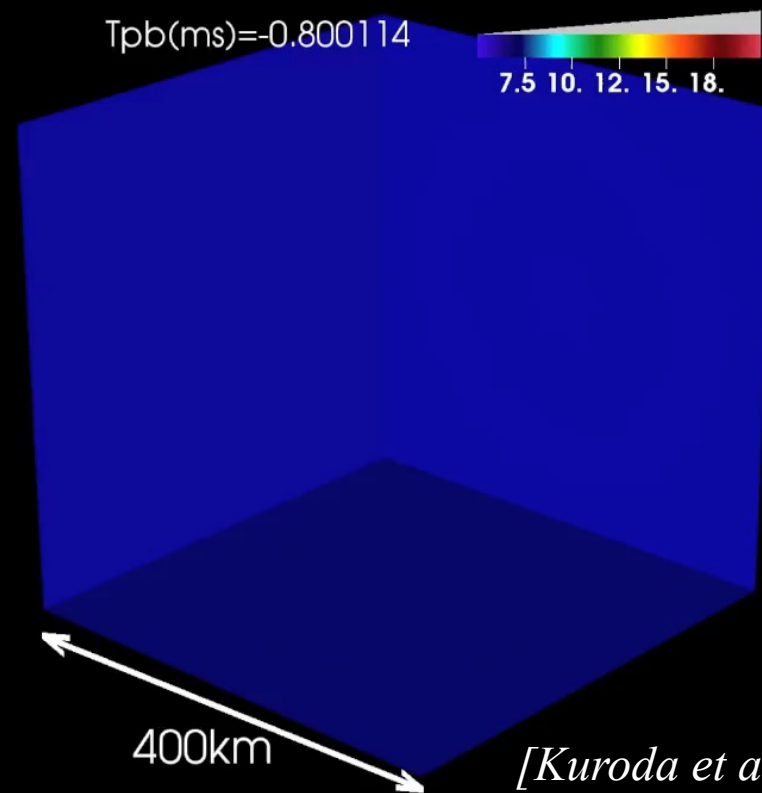
FIG. 1.— In each set of panels, we plot, top; gravitational wave amplitude of plus mode A_+ [cm], bottom; the characteristic wave strain in frequency-time domain \tilde{h} in a logarithmic scale which is over plotted by the expected peak frequency F_{peak} (black line denoted by “A”). “B” indicates the low frequency component. The component “A” is originated from the PNS g -mode oscillation (Marek & Janka 2009; Müller et al. 2013). The component “B” is considered to be associated with the SASI activities (see Sec. 3). Left and right panels are for TM1 and SFHx, respectively. We mention that SFHx (left) and TM1 (right) are softer and stiffer EoS models, respectively.





SFHx :softer

TM1 :stiffer



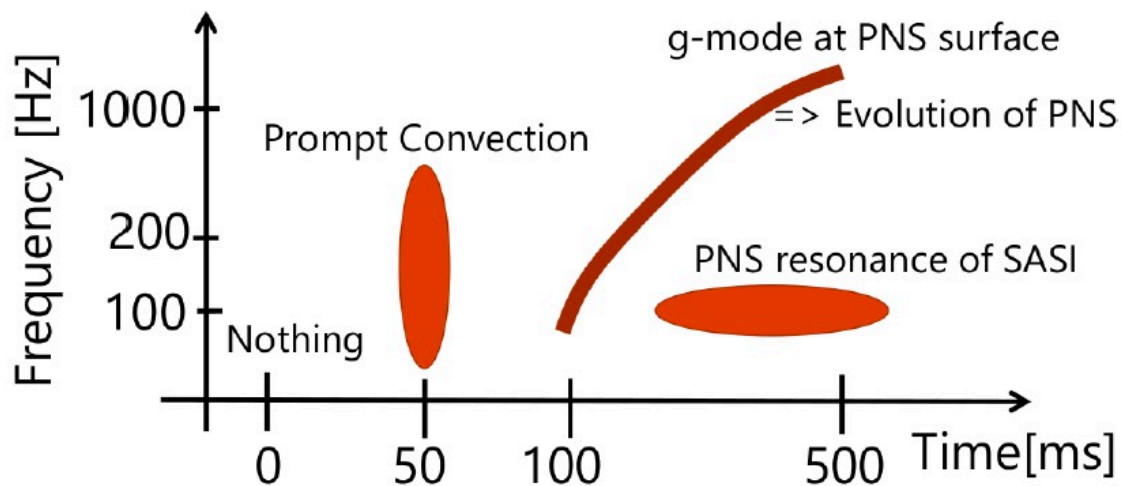
[Kuroda et al 2016, ApJL, 2014, PRD]

✓ **SASI activity higher for softer EOS** (due to high growth rate, e.g., Foglizzo et al. ('06)).

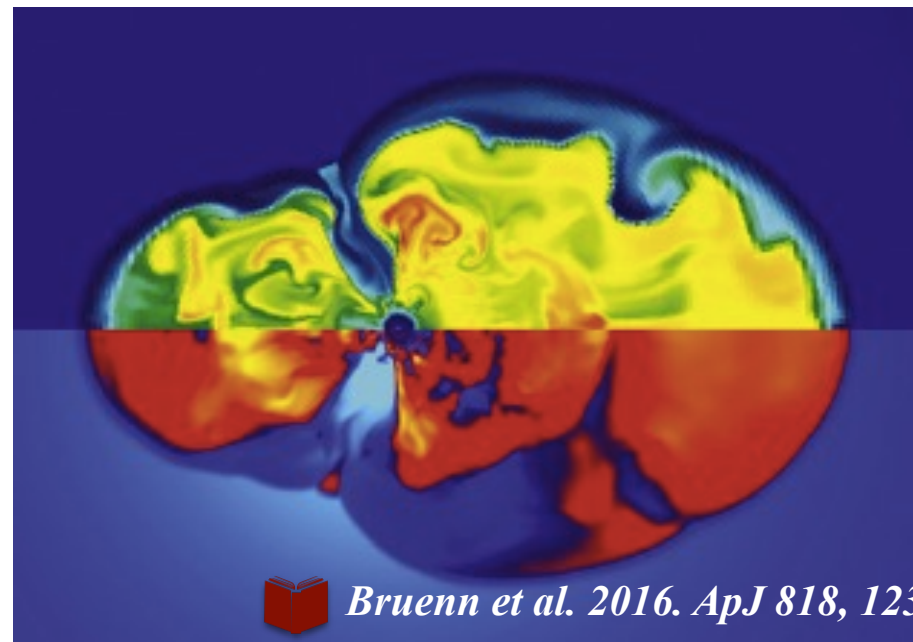
Different scenarios

Neutrino driven CCSNe

Non rotating scenario

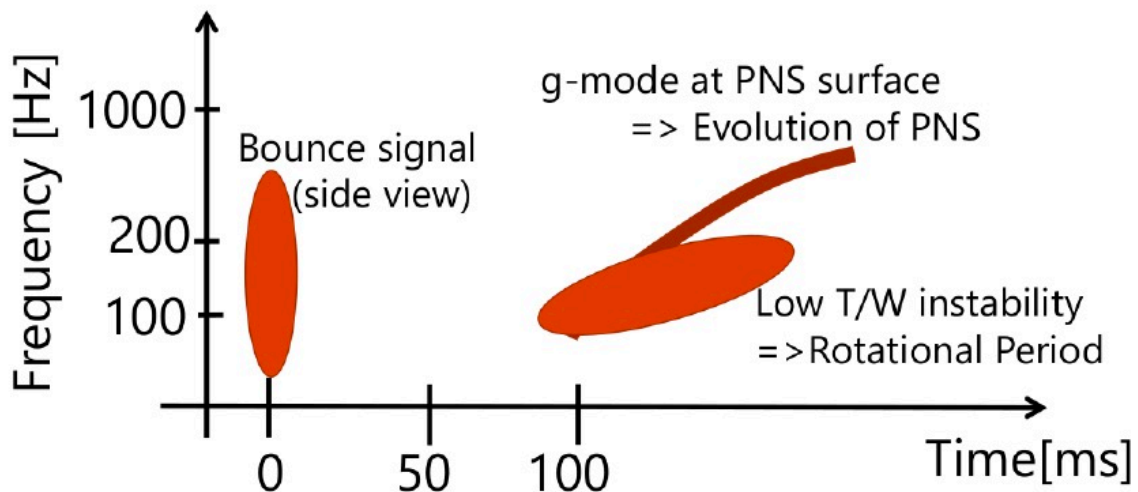


↑ Bounce time is determined by ν observation



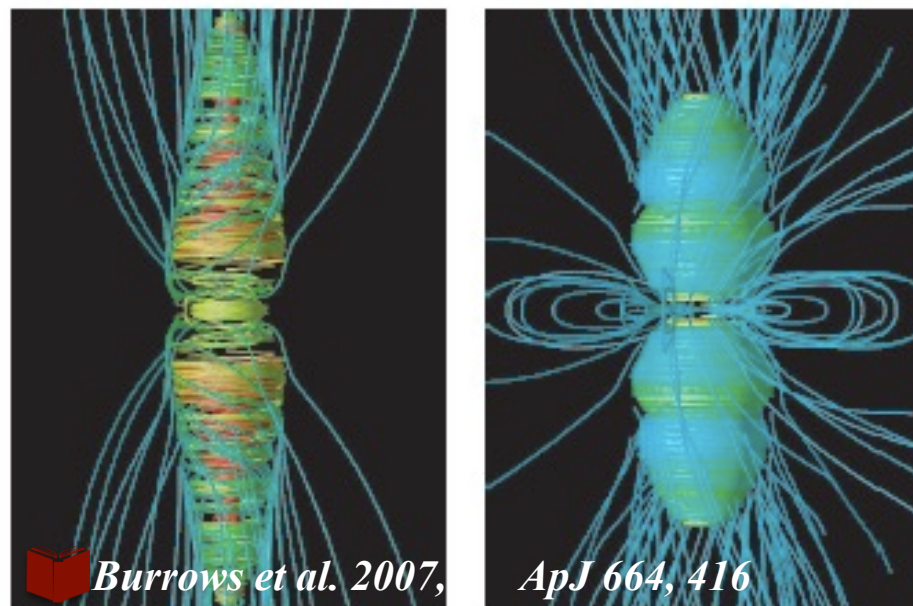
Bruenn et al. 2016. ApJ 818, 123

Rapidly rotating scenario



↑ Bounce time is determined by ν observation

Magneto-rotationally-driven CCSNe



Burrows et al. 2007,

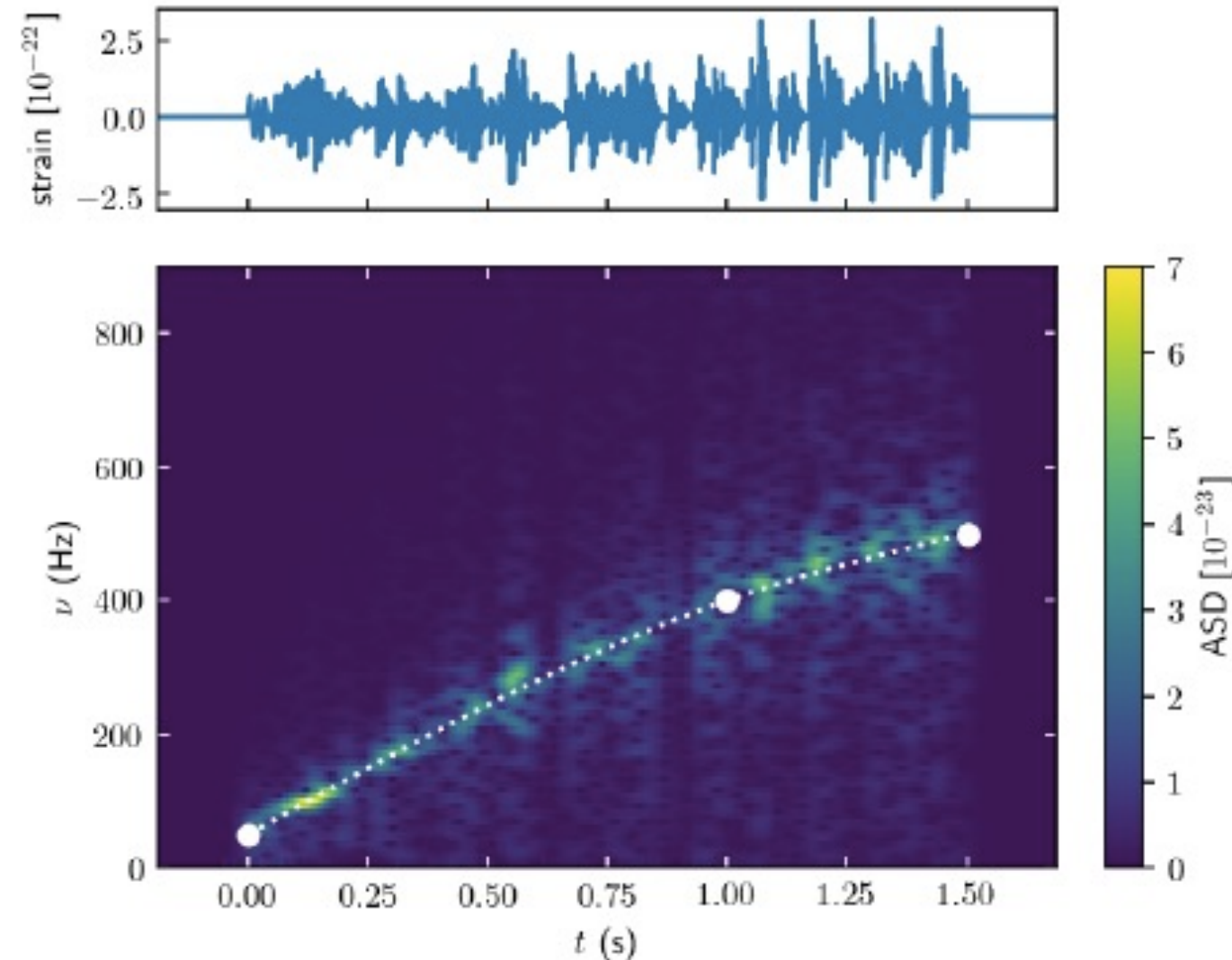
ApJ 664, 416

Credit: Tomoya Takiwaki

Phenomenological Waveforms

- The aim of our phenomenological template is to mimic the raising arch observed in core-collapse simulations.
- The idea is that at each time in the post-bounce evolution, the PNS is in quasi-hydrostatic equilibrium and any perturbation will excite the eigenmodes of the system, in particular g-modes.
- These modes are continually being excited by the hot bubble surrounding the PNS, in particular by convective motions and SASI. At the same time these excited modes are damped by the PNS conditions (e.g. by the existence of convective layers that do not allow for buoyantly supported waves) and by the presence of non-linearities and instabilities (e.g. turbulence).
- The GW emission can be modelled as a damped harmonic oscillator with a random forcing, in which the frequency varies with time.

Phenomenological Waveforms



parameter	min.	max.	Δ	description
t_{ini} [s]	0	0.2	0.1	beginning of the waveform
t_{end} [s]	0.2	1.5	0.1	end of the waveform
ν_0 [Hz]	50	150	50	frequency at bounce
ν_1 [Hz]	1000	2000	500	frequency at 1 s
ν_2 [Hz]	1500	4500	1000	frequency at 1.5 s
ν_{driver} [Hz]	100	200	100	driver frequency
Q	(1, 5, 10)			quality factor
D [kpc]	(1, 2, 5, 10, 15)			distance to source

- New and more flexible parametrisation for the frequency evolution.
- The distance is used as a parameter.



Gravitational Wave Observatories



LIGO, Livingston, LA



LIGO, Hanford, WA



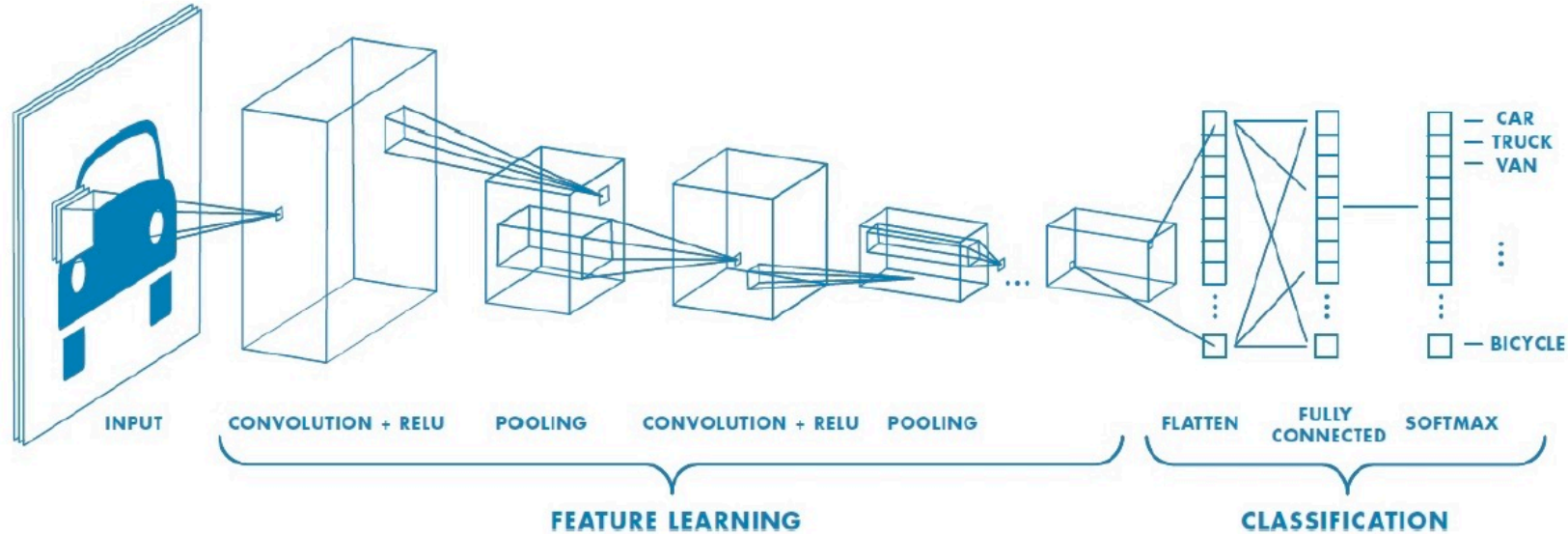
Virgo, Cascina, Italy



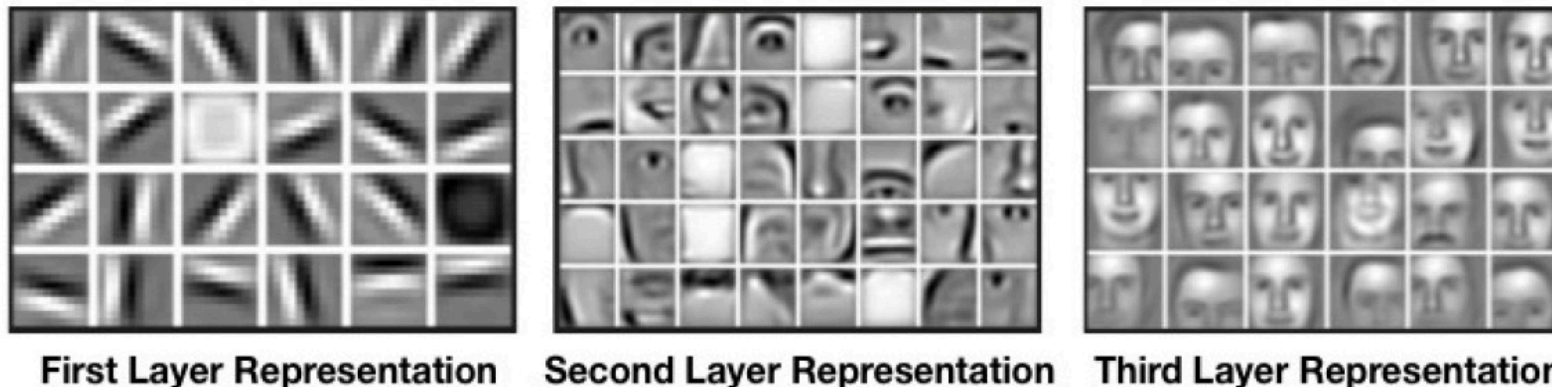
KAGRA, Gifu, Japan

Convolutional Neural Network

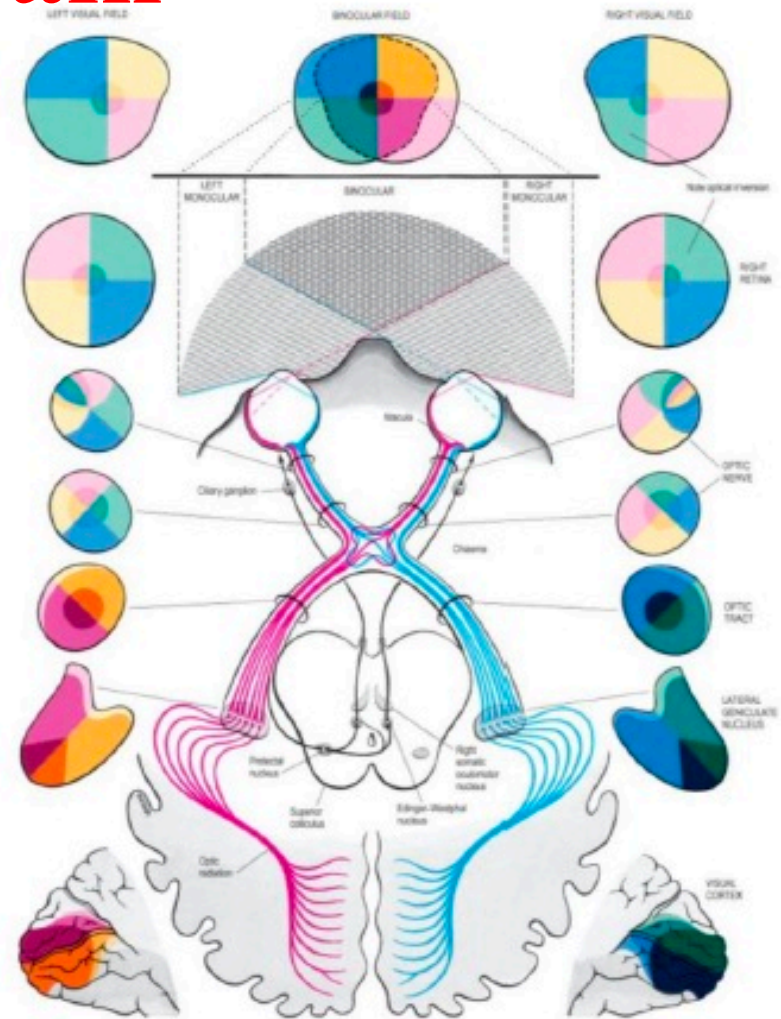
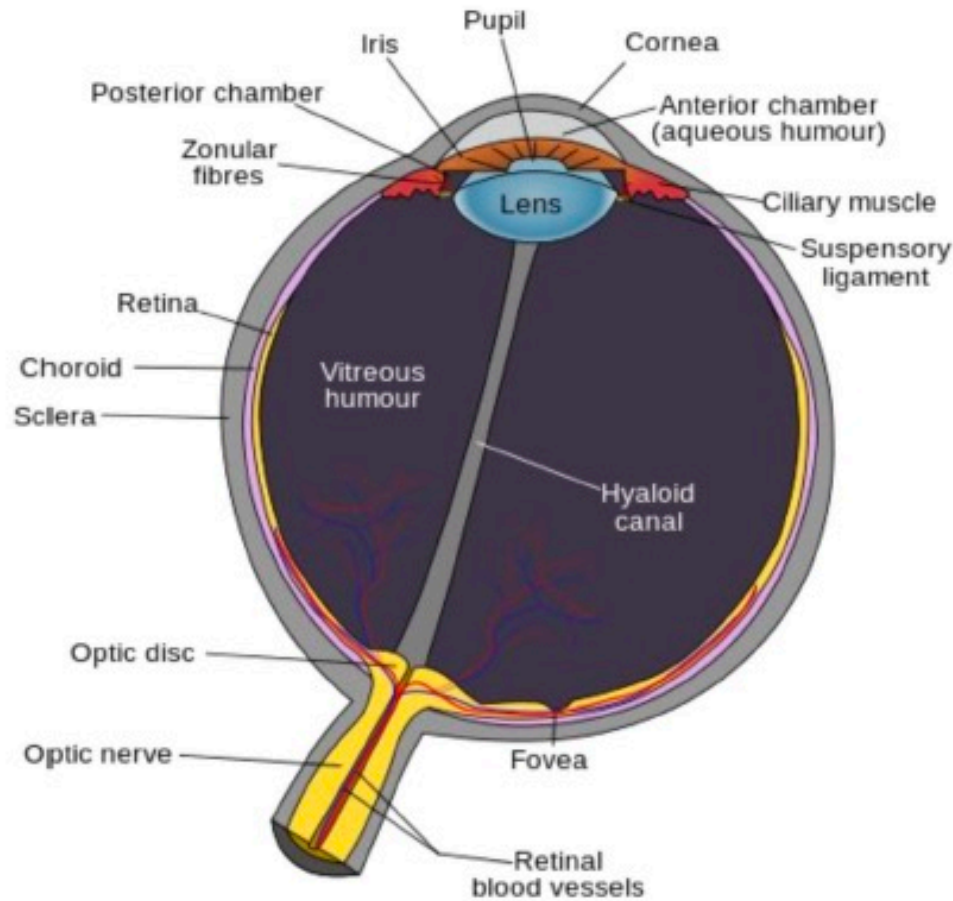
- Convolutional Neural Networks (CNN) are a biologically-inspired trainable architecture that can learn multi-scale hierarchical features.



- This data-driven filter learning provides a visual space decomposition which can be regarded as a hierarchical matched filtering.



Mimic the brain

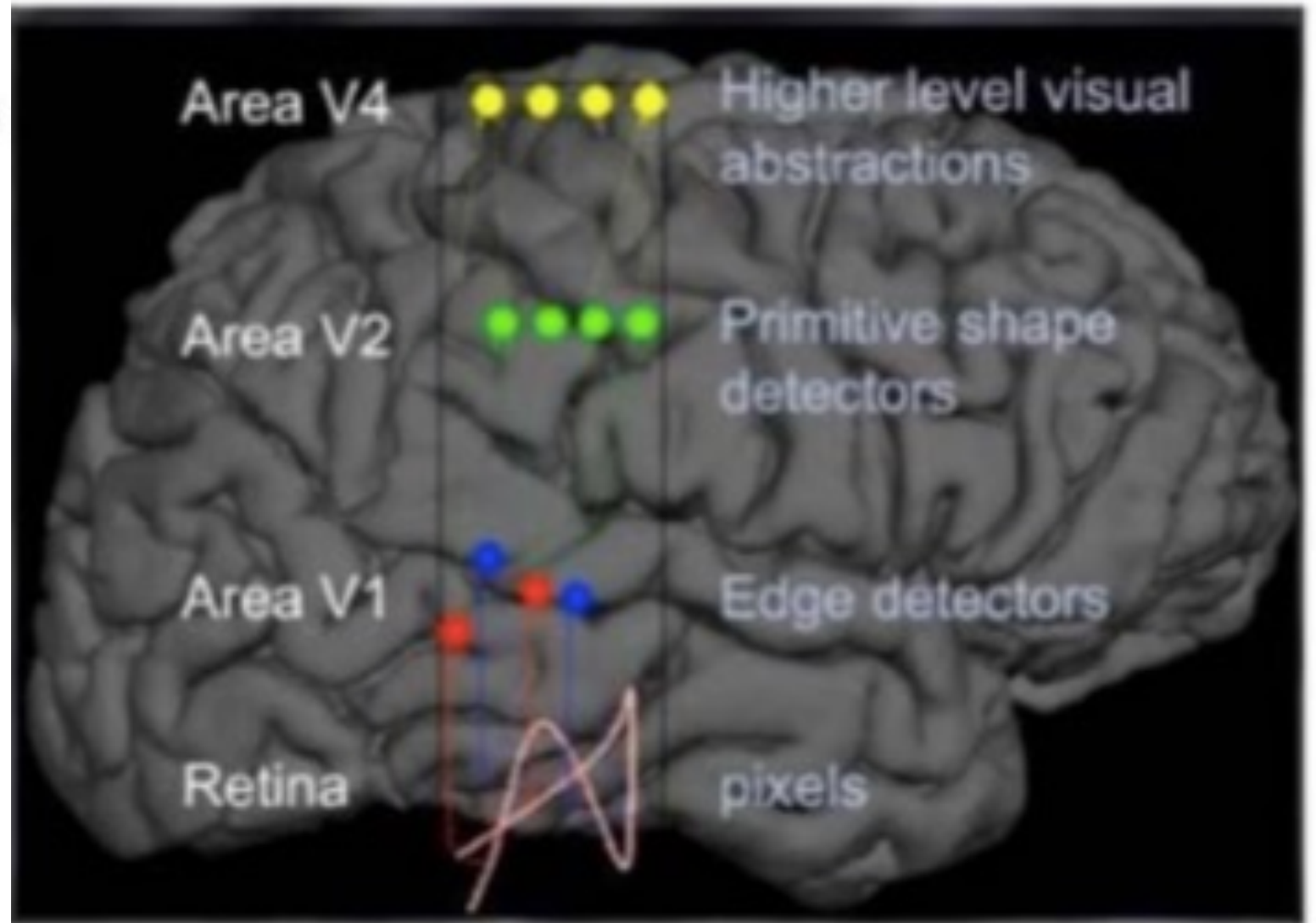
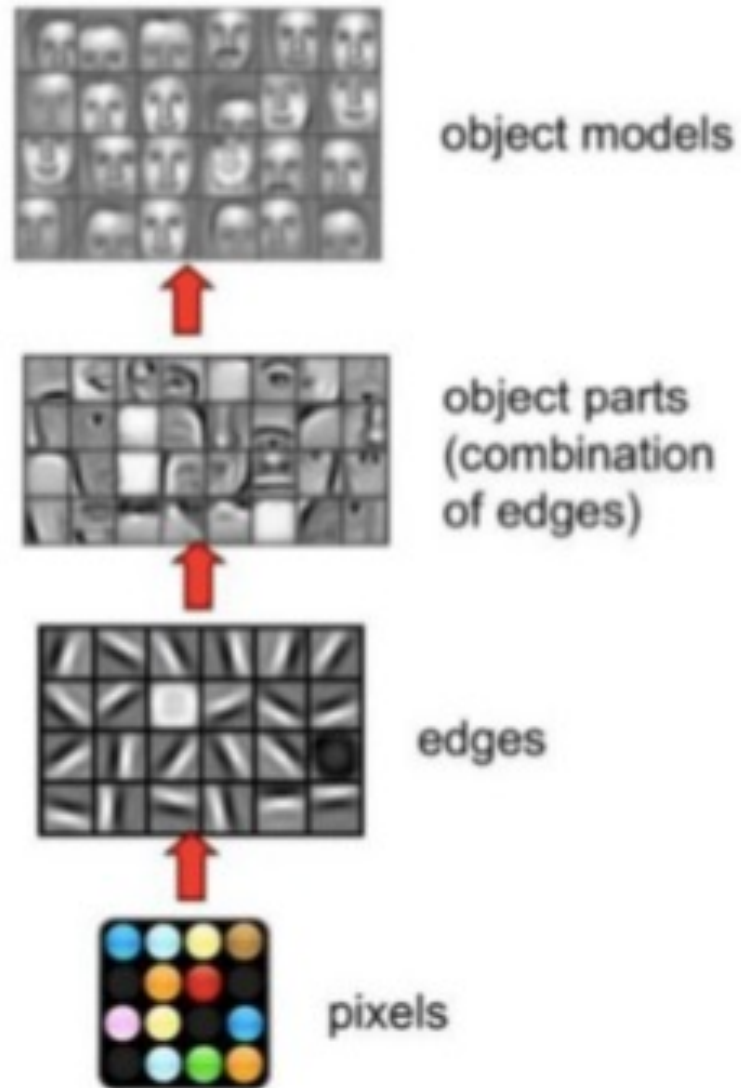


The eye: optical system that creates an upside down image on the retina.

The retina: thin layer of tissue that receives and converts the light into neural signals, and send these signals on to the brain for visual recognition.

The brain: elaborates the data from the retina and builds the final image.

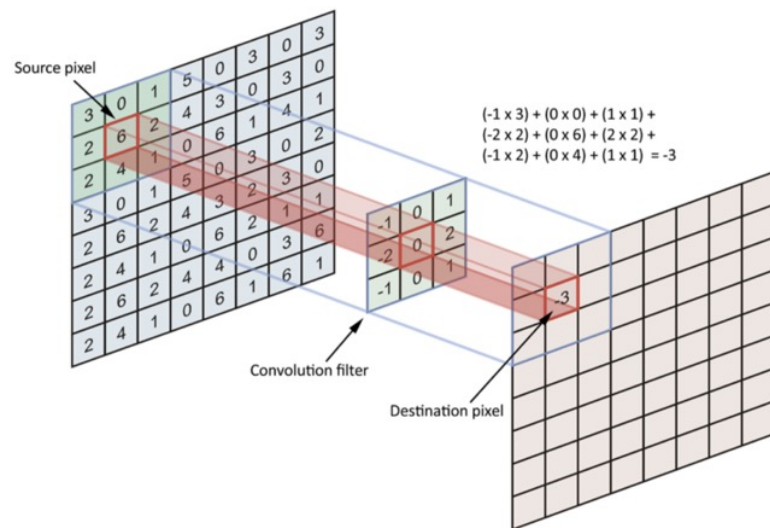
Mimic the brain



Training, Test and Confusion Matrix

The process of achieving the minimisation of the loss function during the **training** stage is the process whereby the machine is “learning”.

For the **test** stage, the CNN will be able to take in input in the form of new data and its output will best represent the probability of that data belonging to each of the trained classes.



The convolution operation.

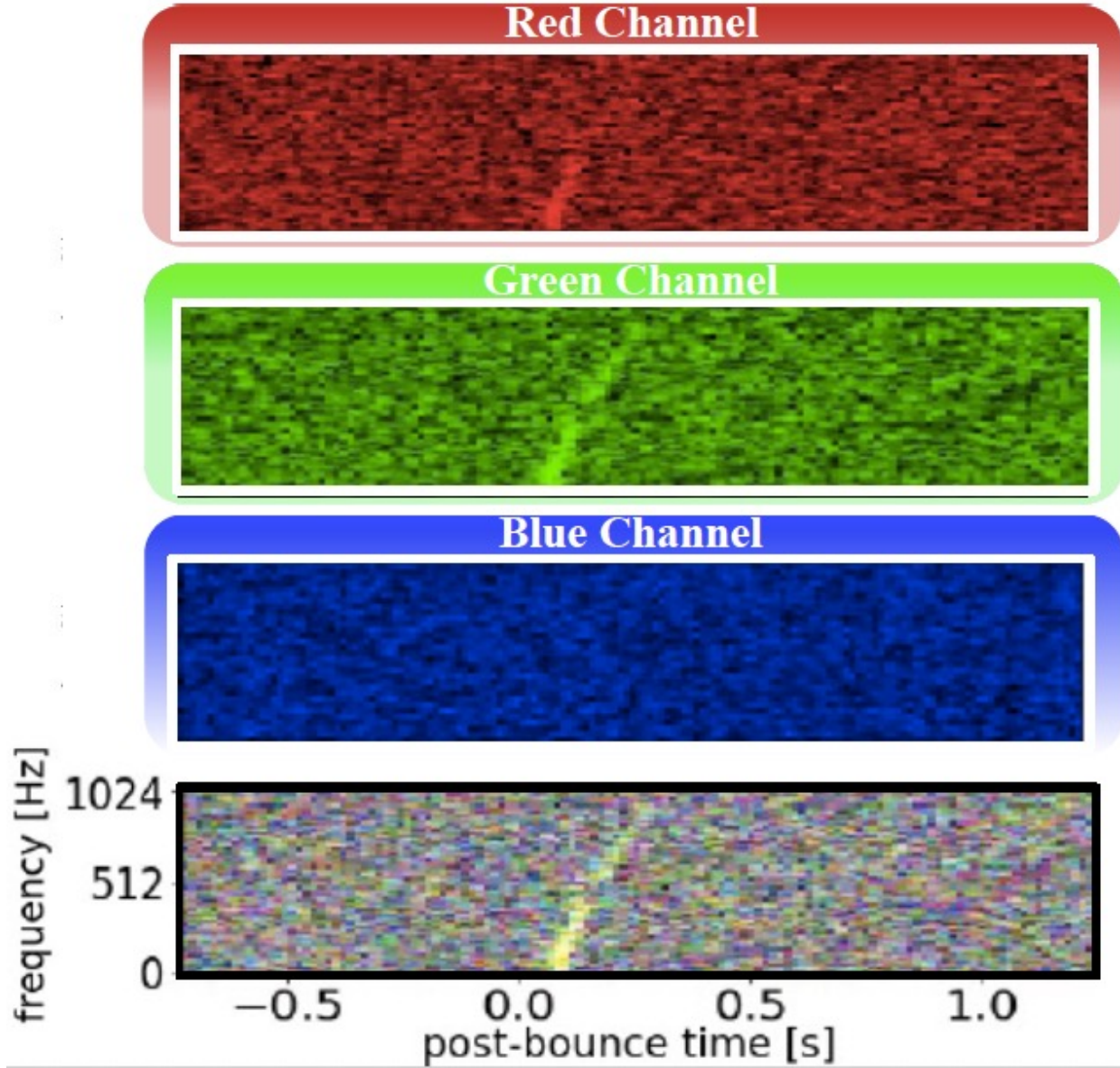
		Predicted Class	
		Positive	Negative
Actual Class	Positive	True Positive (TP)	False Negative (FN)
	Negative	False Positive (FP)	True Negative (TN)

Aim of our Convolutional Neural Network

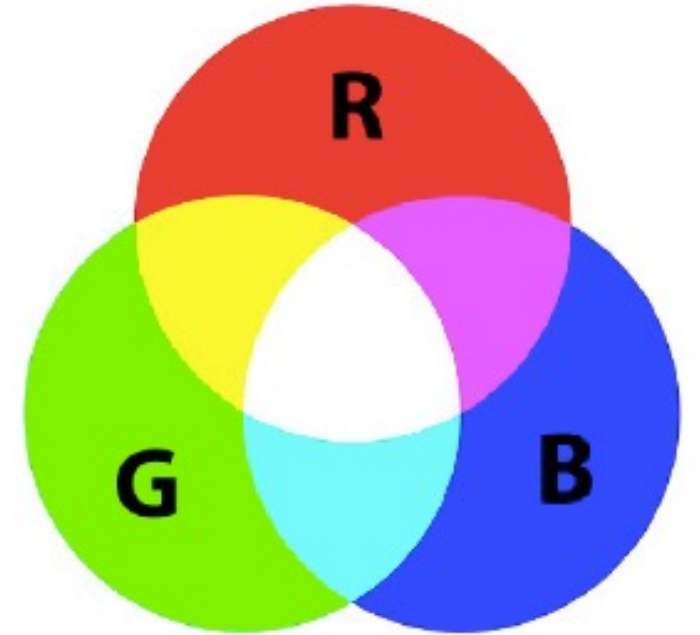
- We want to perform signal detection as an image recognition task, classifying the images in two classes: *Real detector Noise* and *Signal+Real detector Noise*.
- The input images are the RGB multi-detector scalograms.
- The aim is to build a pipeline for a data-driven weakly-modelled robust search.
- Our RGB approach allows us to straightforwardly exploit coincidences among different detectors.

RGB time-frequency plane

Coincidences among detectors



Additive colour synthesis



LIGO Hanford = red

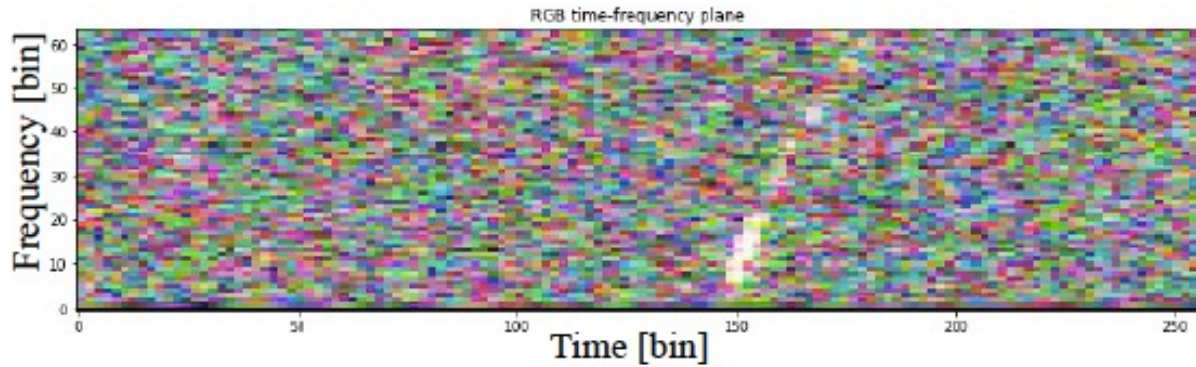
LIGO Livingston = green

Virgo = blue

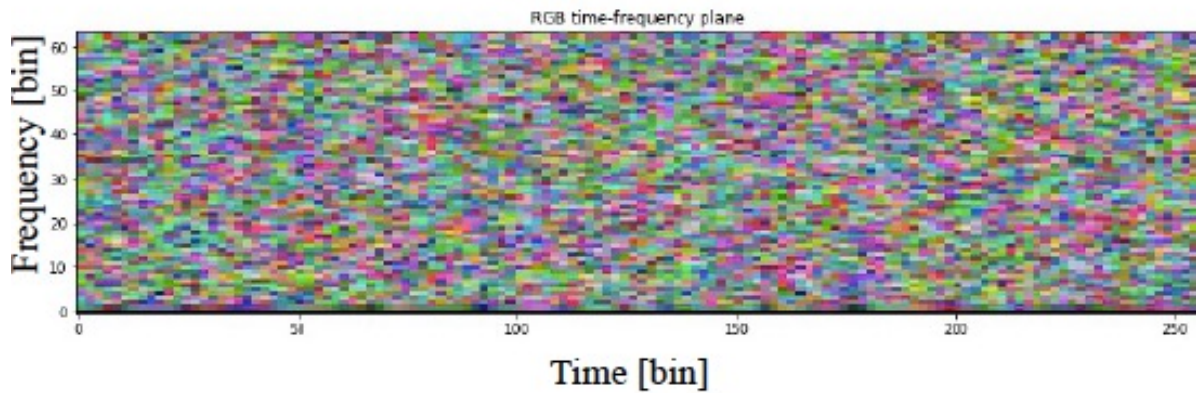
RGB time-frequency plane

Coincidences among detectors

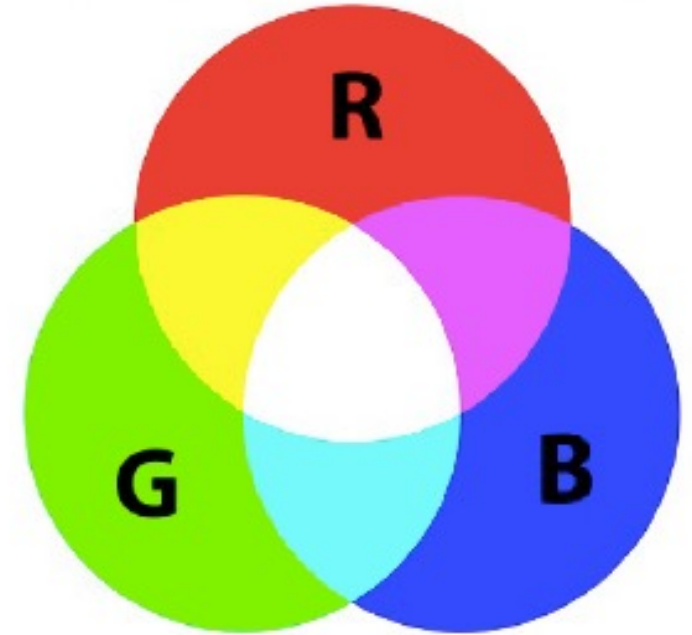
Signal+Noise



Only Noise



Additive colour synthesis



LIGO Hanford = red

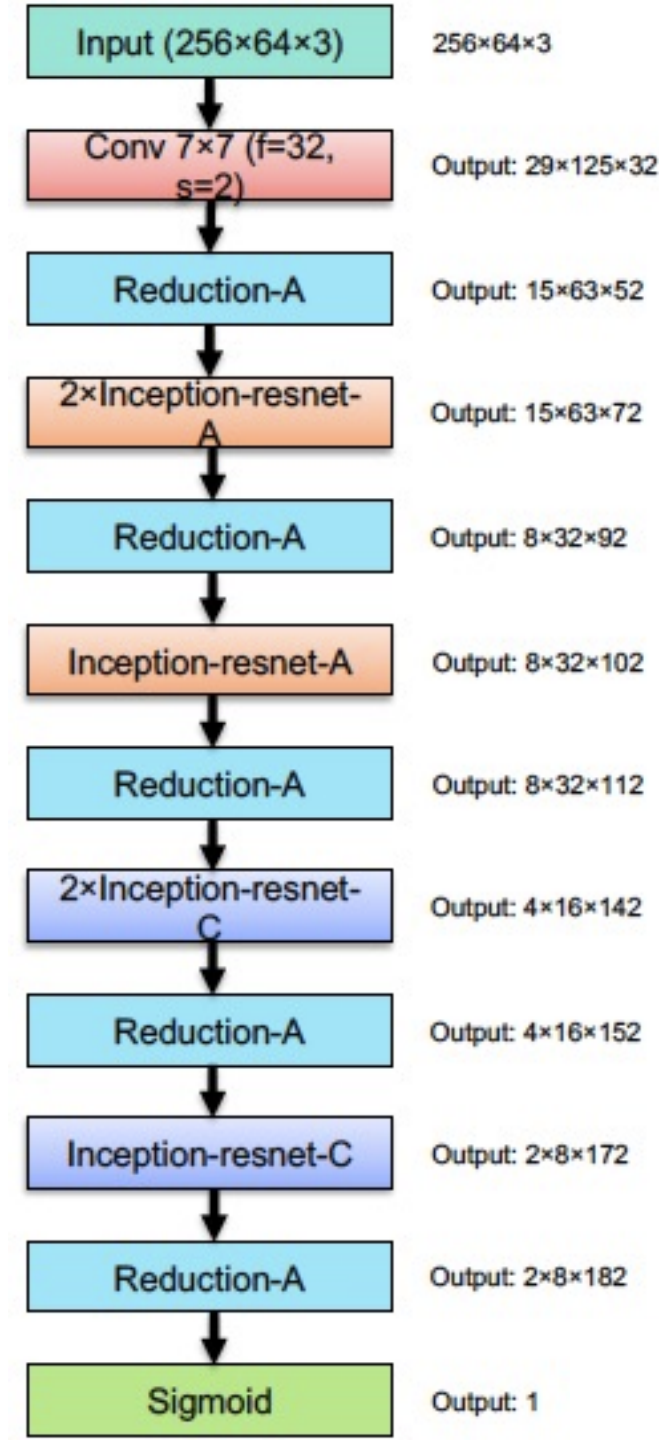
LIGO Livingston = green

Virgo = blue



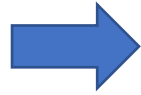
Architecture of the deep learning algorithm

- Mini Inception Resnet v1: reduced version of Inception-Resnet
- Keras framework, based on the TensorFlow backend
- Total number of parameters: 98997
- 30 times more complex than previous network
- The task is treated as a multi-class classification problem with two classes: the event class and the noise class, by using the binary cross entropy.
- The training and validation phase, performed in the real detector noise, is done in 2 h and 21 min using a GPU Nvidia Quadro P5000, while predicting the test set takes 3 ms for each 2 s long image.



Data: from Gaussian noise to real noise

Gaussian noise
(Previous work)



Previous set: 10^4 images for each value of Network SNR $\in [8,40]$

Real noise

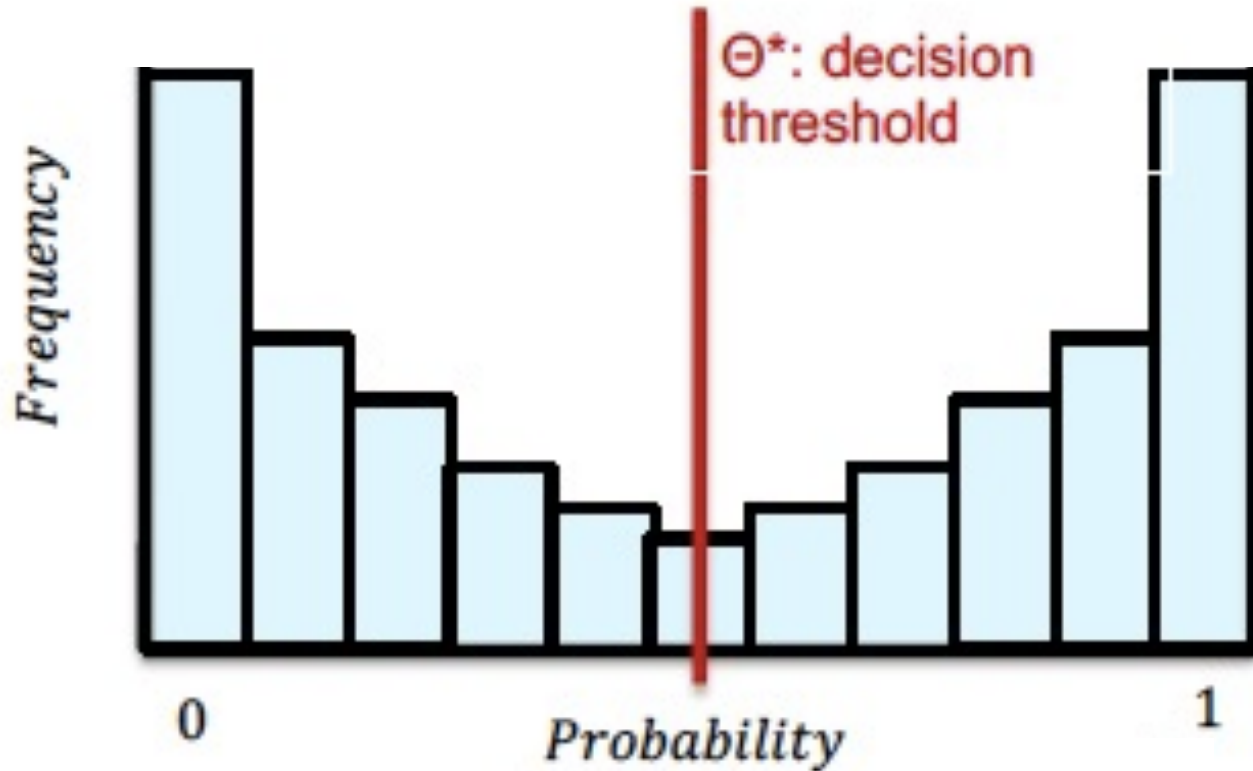
(O2 – August 2017)

- **Training set – phenomenological waveforms:** 7×10^4 images for each distance $\in [0.2, 3]$ kpc and random sky localisation.
- **Blind set – phenomenological waveforms:** 26×10^4 images with distances chosen in a uniform distribution $\in [0.2, 15]$ kpc. NOT involved in the training or validation procedure.
- **Test set - numerical simulations from the literature:** 6.5×10^4 images with distances $\in [0.1, 15]$ kpc

In particular, we chose a stretch of real data even containing glitches, taken during August 2017, when Virgo joined the run. The period includes about 15 days of coincidence time among the three detectors and we used this data set to generate about 2 years of time-shifts data to train and test the neural network as noise class.



Measuring and constraining the learning



- The output of the network is a probability vector ϑ , which contains the probabilities of the template belonging to one class or another.
- The classification task is performed according to a threshold ϑ^* , the template will be classified as event class only if its probability overcomes ϑ^* .

Confusion matrix

		Actual class	
		<i>Event</i>	<i>Noise</i>
Predicted class	<i>Event</i>	True positive (TP)	False positive (FP)
	<i>Noise</i>	False negative (FN)	True negative (TN)

Efficiency:

$$\eta_{CNN} = \frac{\text{correctly classified signals}}{\text{all the signals at CNN input}} = \frac{TP}{TP + FN}$$

False Alarm Rate:

$$FAR_{CNN} = \frac{\text{misclassified noise}}{\text{all classified events}} = \frac{FP}{FP + TP}$$

False Positive Rate:

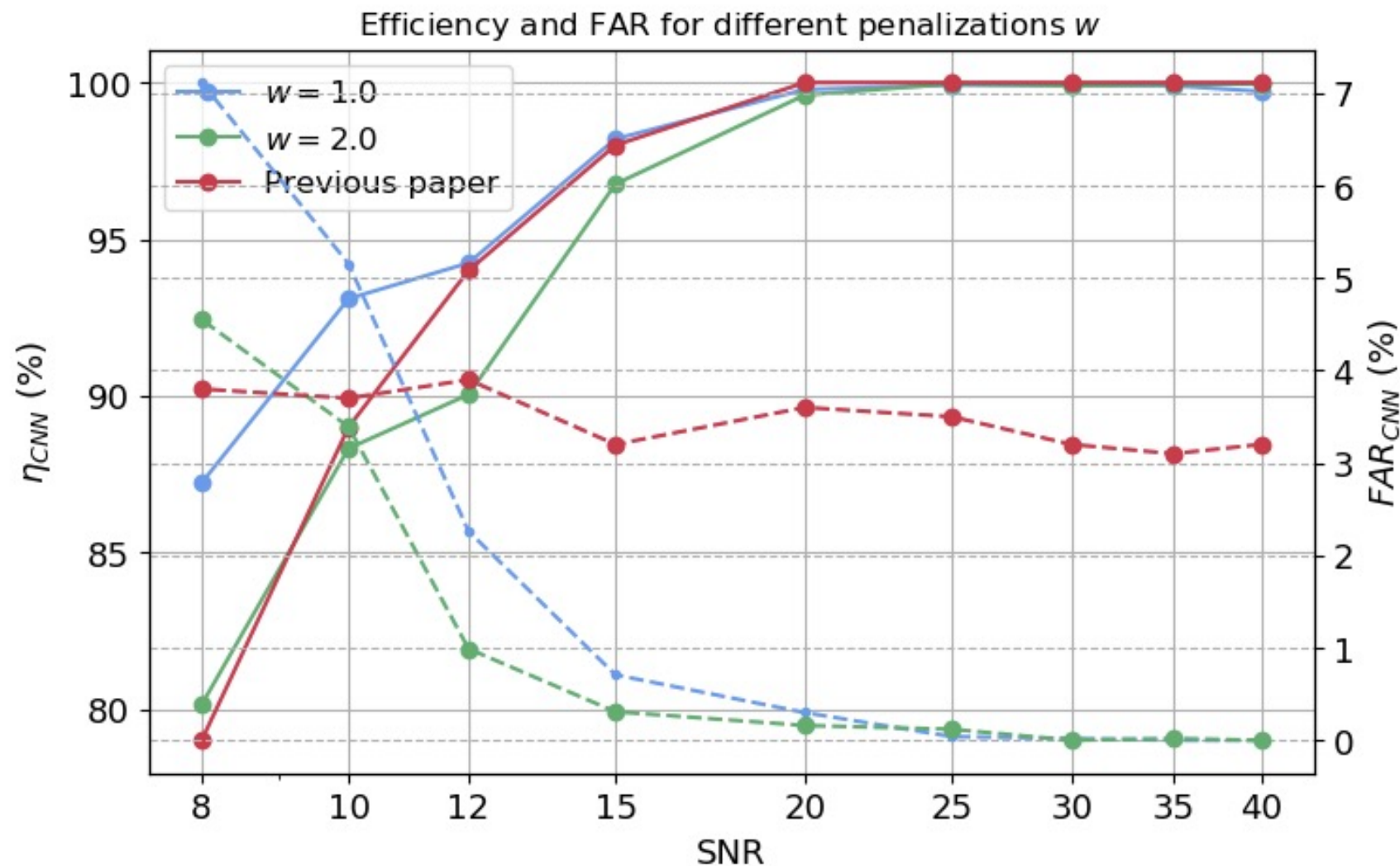
$$FPR = \frac{FP}{FP + TN}$$

Comparison with previous work in Gaussian noise

Weighted binary cross-entropy:

$w=1$ correctly classify the noise class or the event class is the same

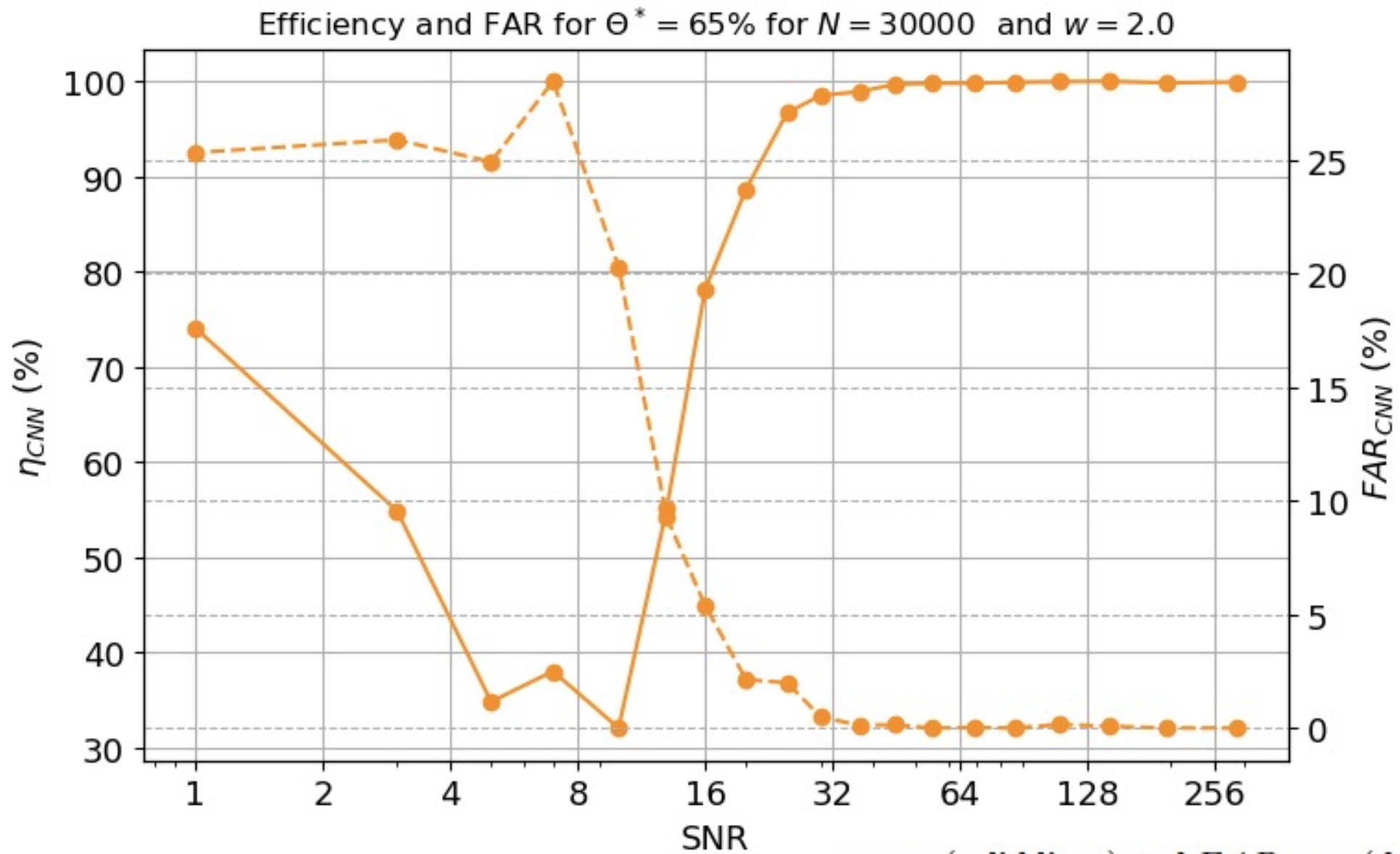
$w=2$ it is 2 times more important to correctly classify the noise class rather than the event class.



η_{CNN} (solid lines) and FAR_{CNN} (dashed lines)



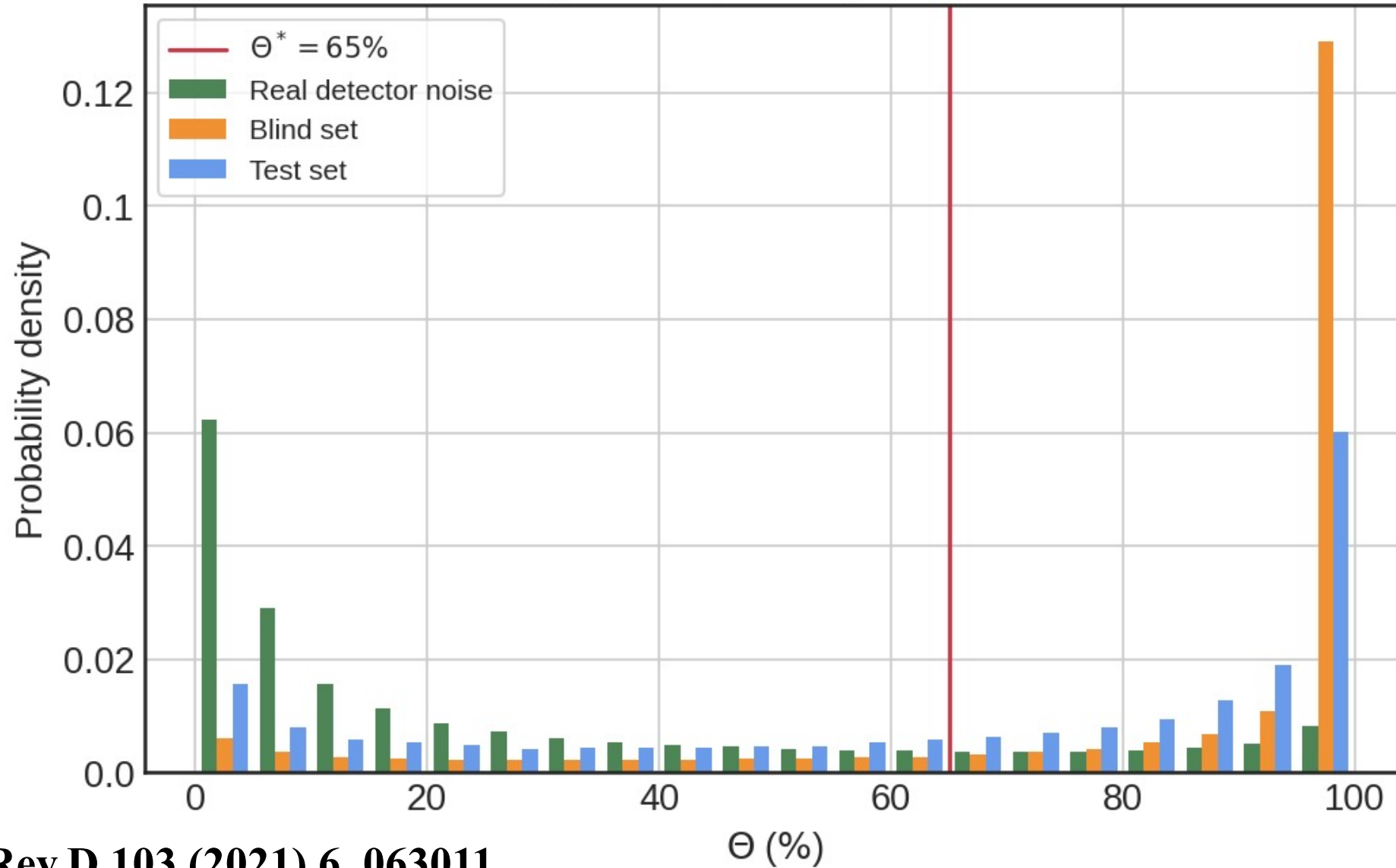
Validation process in real detector noise



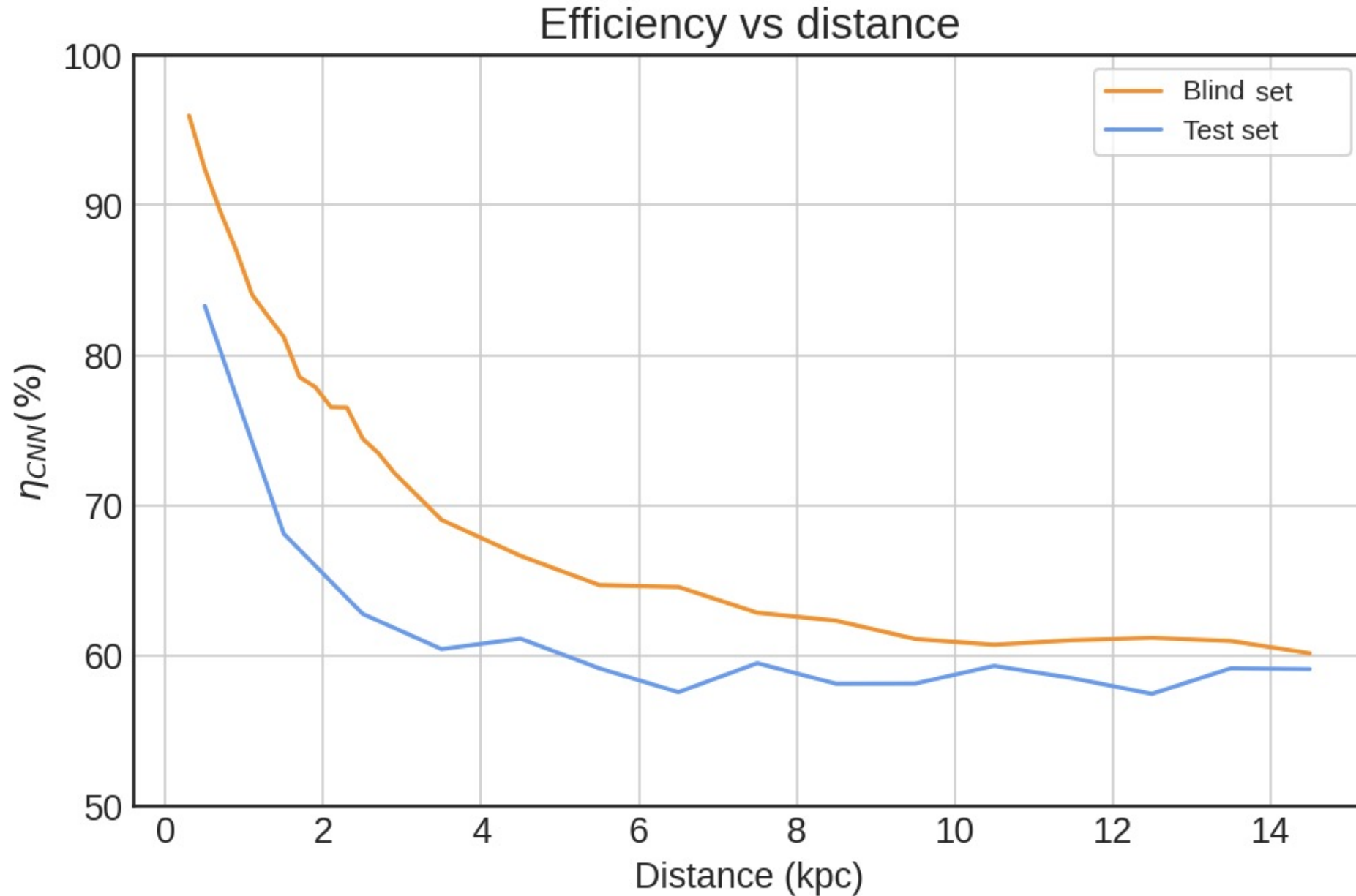
η_{CNN} (solid lines) and FAR_{CNN} (dashed lines)

Results in real detector noise

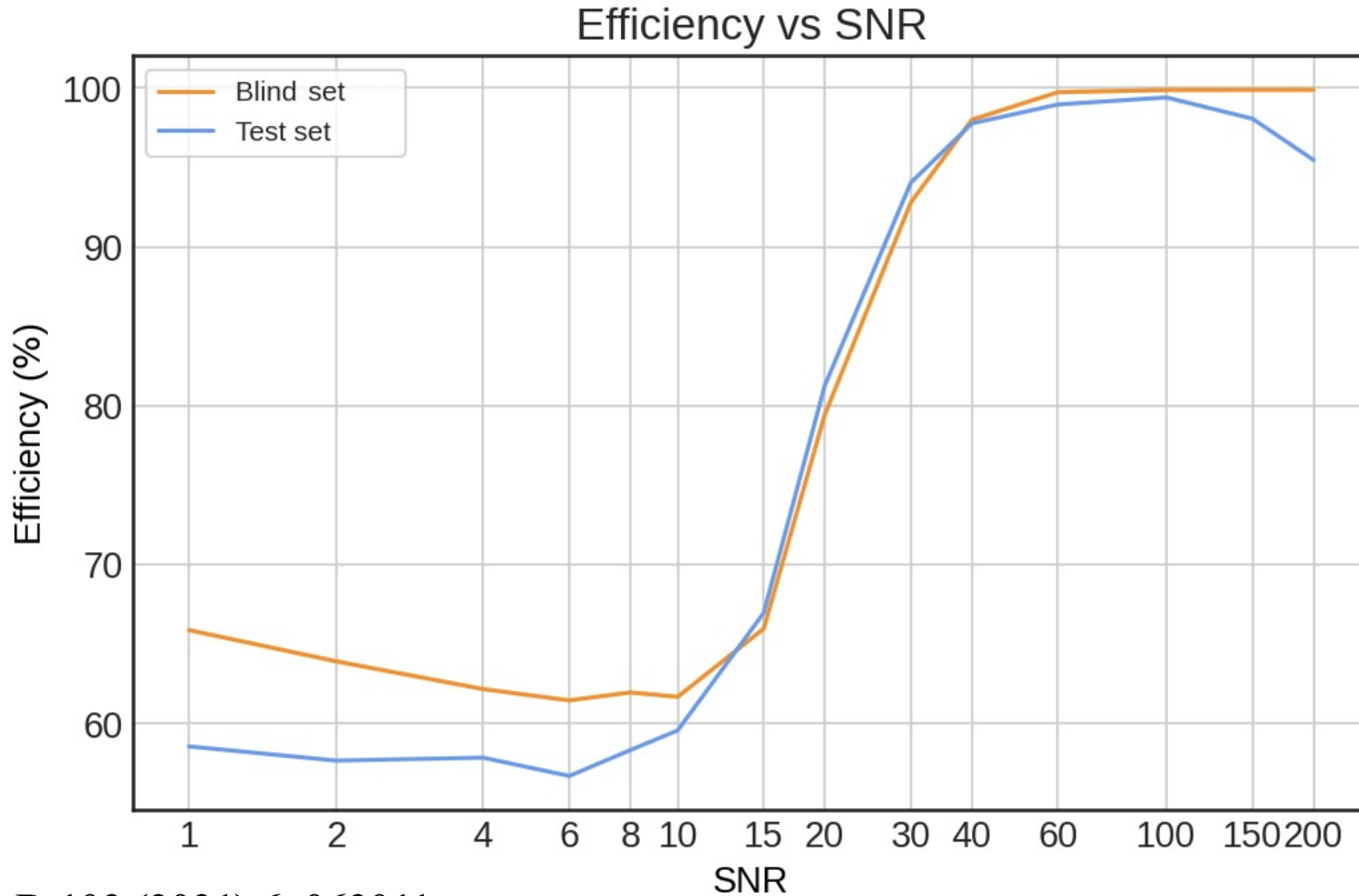
Probability density histogram for $w = 2.0$



Results in real detector noise



Results in real detector noise



Conclusions

- We trained a newly developed Mini-Inception Resnet neural network using time-frequency images corresponding to injections of simulated phenomenological signals, which mimic the waveforms obtained in 3D numerical simulations of CCSNe.
- We computed the detection efficiency versus the source distance, obtaining that, for signal to noise ratio higher than 15, the detection efficiency is 70 % at a false alarm rate lower than 5%.
- In the case of O2 run, it would have been possible to detect signals emitted at 1 kpc of distance, whilst lowering down the efficiency to 60%, the event distance reaches values up to 14 kpc.
- These results are very promising for future detections and the algorithm has multiple possible extensions.

